Fullerene (C60) nanowires: the preparation, characterization, and potential applications

DR. XH XIA (Orcid ID : 0000-0002-1332-9310)

DR. JUNFENG GENG (Orcid ID : 0000-0001-6246-0342)

Article type : Review

Fullerene (C_{60}) nanowires: the preparation, characterization, and potential applications

Xiao Fan,[1] Navneet Soin,[1,5] Haitao Li,[2] Hua Li,[3] Xiaohong Xia,[4] and Junfeng Geng[1]*

[1]*Institute for Materials Research and Innovation, & Institute for Renewable Energy and Environmental Technologies, University of Bolton, Bolton, BL3 5AB, UK*

[2]*School of Chemistry and Chemical Engineering, Jiangsu Normal University, 101 Shanghai Road, Xuzhou, 221116, China*

[3]*College of Life and Environmental Sciences, Minzu University of China, Beijing, 100081, China*

[4]*School of Materials Science and Engineering, Hubei University, Wuhan, 368 Youyi Road, 430062, China*

5*School of Engineering, Ulster University, Newtownabbey, Belfast, BT37 0QB, Northern Ireland, UK*

*Corresponding author email: j.geng@bolton.ac.uk

Abstract: Fullerene (C_{60}) nanowires have attracted significant attention in the past two decades due to their outstanding chemical and physical properties, which render the material a wide range of potential applications. Much effort has been devoted to exploring the growth methods, structural and compositional characterizations, as well as application-related investigations of this novel carbon nanomaterial. Here we present a review of C_{60} nanowires in which we will first describe the recent development in the materials preparations, analytical techniques, crystal structures, chemical compositions, and the investigations of polymerization processes. Afterwards, we will discuss the mechanistic studies on the nanowires' growth as the mechanism research is of great importance for their size control, large-scale preparation, and for the exploration of applications in a wide range of fields.

This article has been accepted for publication and undergone full peer review but has not been through the copyediting, typesetting, pagination and proofreading process, which may lead to differences between this version and the Version of Record. Please cite this article as doi: 10.1002/EEM2.12071

Finally, we will discuss the potential applications in several directions, including optical, electrical, mechanical and biological fields, as well as our perspectives to future developments.

Key words: fullerene, C_{60} nanowires, nanowire science, nanotechnology

1. Introduction

Fullerene (C_{60}), first discovered in 1985 by researchers at the University of Rice,[1] has attracted considerable scientific and technological attention owing to its unique physical, chemical and biological properties with possible applications in areas as diverse as optoelectronics,[2] solar cells,[3] optical limiters,[4, 5] sensors,[4] luminescent devices,[6] optical filters,[6] and virucidal compounds,[7-9] *etc*. A C_{60} molecule, with a nuclear framework diameter of 7.1 Å, shows a truncated icosahedron structure. It consists of 60 carbon atoms located at the nodes of 20 hexagons and 12 pentagons which are arranged in a cage-like lattice, and the structure is defined by alternating single and double bonds.[10, 11] Since C_{60} molecules are small, isotropic and spherical, they can be regarded as an ideal zero-dimensional (0D) building units allowing for a subsequent construction of higher-dimensional structures *i.e.* 1D, 2D and 3D nanomaterials to realize some important aspects of nano-architectonics.[11] The solubility of fullerenes in common organic solvents, such as toluene, carbon disulfide, dicholobenzene *etc.*, is good, and a large industrial scale synthesis of high purity and size-controlled fullerenes is now possible with various products on the market.

Among the various crystalline forms of fullerenes, C_{60} nanowires, as 1D nanostructure of C_{60}, are of particular interest owing to their outstanding properties and potential applications resulting from their high surface area, low-dimensionality, and potential quantum confinement effect,[4, 10, 12] as well as the possibility of serving as 1D building units in magnetic and photonic applications.[13, 14] There have been a number of reports on the growth, structural characterization, and application-related investigations of C_{60} nanowires. In this review, we highlight the recent development and provide future outlooks in the research area. The potential applications of the material could be many, which include optical limiters[4, 5] photoconductors for solar energy devices,[2] fuel cells,[6] field-emission transistors,[15, 16] nanoprobes,[17] high frequency filters,[17] and targeted drug-delivery vehicles,[18-20] *etc*, and these applications are also discussed in this paper.

2. Preparation of C_{60} nanowires

There are currently two ways used for preparation of C_{60} nanowires: the direct solution growth method and the liquid-liquid interfacial precipitation (LLIP) method. The direct solution growth may be undertaken by slowly evaporating organic solvent in a saturated C_{60} solution to allow C_{60} crystals growth. Incorporation of solvent molecules into the crystal lattices leads to different crystalline forms including needle-like and nanowire-like

C_{60} crystals. The volume of the unit cell has been demonstrated to increase with the increase of the molecular size of the solvent.[10] Different from this, a LLIP method would need to use two solvents and C_{60} nanowires will grow at the liquid-liquid interface of the two solvents. The LLIP method may be modified by varying the solvents, solvent amount ratio, and the illumination conditions, *etc*.[17, 21-26]

2.1 Direct solution growth method

Ogawa and co-workers observed the assembly of C_{60} from toluene solution and prepared huge needle-like structures of C_{60} crystals with high aspect ratios by slow evaporation of non-electrolysis supersaturated solutions of C_{60} in toluene over a period of about 6 months.[27] The size of the crystals was quite diverse ranging from micrometres to few tens of millimetres in length with diameters of up to ~10 μm (Figure 1(a)). Besides these huge crystals, ultra-fine wire-like crystals as small as 50 nm in width were also observed (Figure 1(b)). These ultra-fine nanowires were considered to have the same structure as in the needle-like crystals.[27]

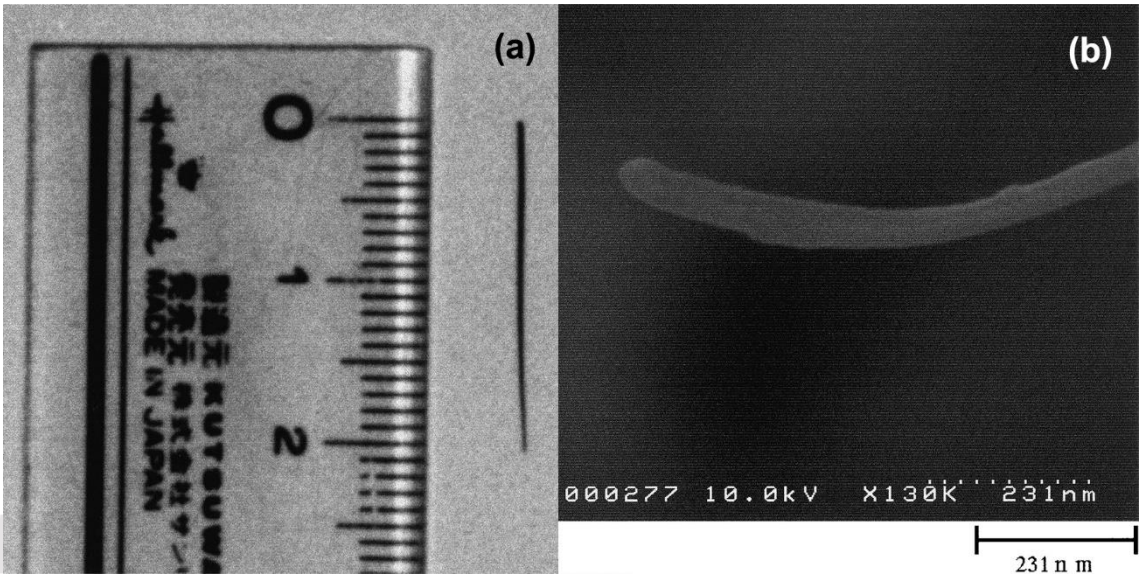

Figure 1. (a) A large needle-like C_{60} crystal obtained by very slow evaporation of the toluene solution of C_{60}; (b) SEM image of an ultra-fine nanowire in the needle-like crystal sample.[27]

Wang *et al.* prepared individual C_{60} nanowires on silicon and glass substrates by evaporation of C_{60}-saturated m-xylene solution at room temperature over a period of 2 hours.[19] A heat treatment was then performed on these C_{60} nanowires with a tubular furnace at 150 °C under vacuum condition for 5 hours. The length and diameter of these C_{60} nanowires were typically ~100 μm and 100-450 nm, respectively. Most of them were 200 nm in diameter while the thinnest nanowires had widths smaller than 30 nm. As shown in Figure 2, these C_{60} nanowires were grown on substrate, which made them potentially suitable for applications in nanoscale devices.[28]

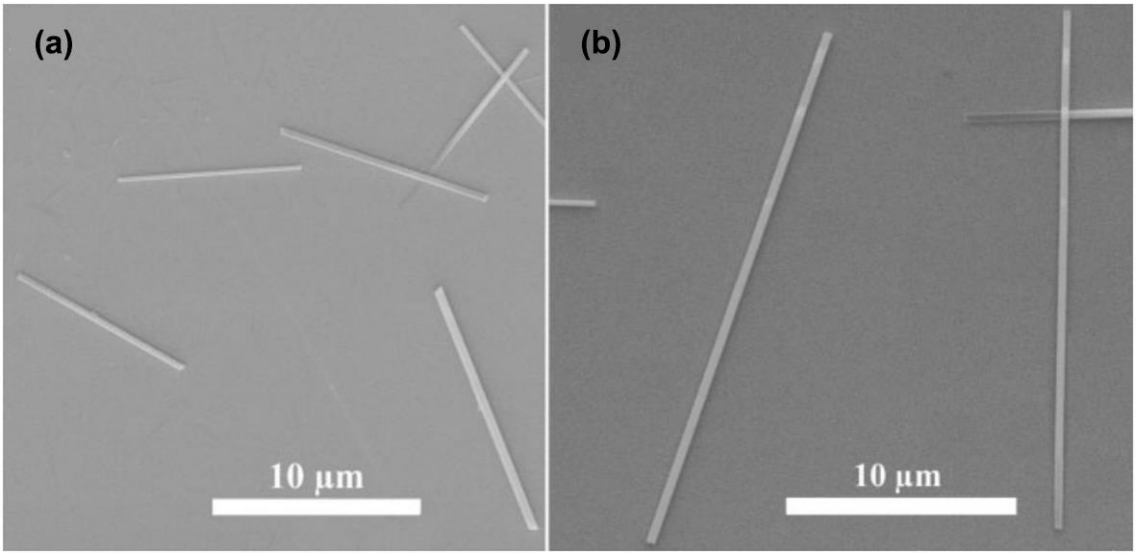

Figure 2. SEM images of C_{60} nanowires prepared by evaporating 0.1 mL of the saturated C_{60} m-xylene solution on silicon substrates (1 cm × 1 cm) for (a) 1 h and (b) 1.5 h.[28]

Yao *et al.* employed a similar method to prepare C_{60} nanowires on substrates wherein o- (ortho-), m- (mata-), p- (para-) dichlorobenzene, m-, p-dibromobenzene and m-, p-diiodobenzene were used as solvents and a variety of substrates including silicon, glass and aluminium foil were employed.[29] Fullerene nanowires obtained from the C_{60}-saturated m-dichlorobenzene solutions on a silicon substrate were observed to have a hexagonal-shaped cross section and a broad width distribution ranging from tens of nanometres to several micrometres, while the two most dominant width distributions were within the ranges 100-600 nm and 1-2 mm. The length-to-width aspect ratios of these C_{60} wires varied from 10 to more than 500 and can be adjusted by changing the concentration of C_{60} in solution. Different from the results from Wang's report,[28] C_{60} nanowires were grown either separately or interlaced on the substrate. By comparing the growth using different solvents, it was observed that the meta-type solvents, which are aromatic compounds with substituents at 1 and 3 positions, are efficient for the C_{60} nanowires while no wire-like crystals were obtained by using ortho- and para-type solvents. The chemical affinity of the aromatic solvent molecules to C_{60} may contribute to the formation of wire-like C_{60} crystals.[29]

Geng *et al.* prepared long C_{60} nanowires by slow evaporation of solutions of high-purity C_{60} powder (99.9%) in 1,2,4-trimethylbenzene (1,2,4-TMB) at room temperature (Figure 3). These C_{60} nanowires were typically 100-500 nm in diameter and 200-1000 μm in length, with some of the nanowires as long as 1.5 mm, therefore, the largest length-to-width aspect ratio reached ~3000.[10] The solution was aged in a glass vial which was loosely covered with a plastic plate on the top. With the slow evaporation of solvent, an abundant growth of cotton-like nanowires with a golden-brown colour was found on the upper internal wall and around the mouth area of the vial. The morphology of these C_{60} nanowires was found to be quite unusual, with each nanowire being composed of a prism-like central core and two or three nanobelts joined along the growth direction to give a V- or Y-shaped cross section.[10, 30]

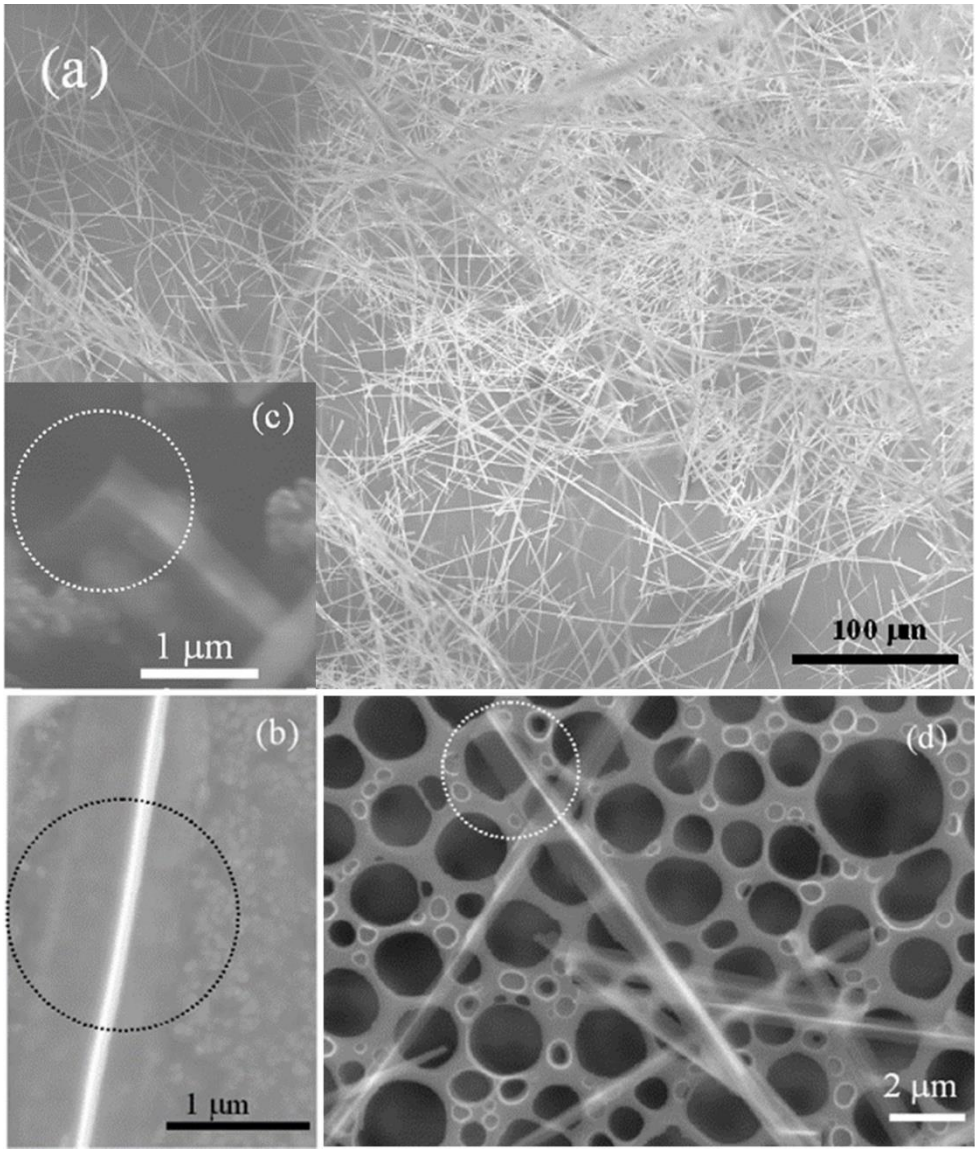

Figure 3. (a) SEM image of the overall morphology of the C_{60} nanowires prepared by evaporation of C_{60} solution in 1,2,4-trimethylbenzene. (b) SEM image of a single nanowire with the two component nanobelts along the crystal ridge. (c) SEM image of the V-shaped end of the nanowire together with the crystal ridge. (d) TEM image of the V-shaped cross section and the two component nanobelts within each nanowire.[10]

Zhou and co-workers prepared C_{60}/1,3,5-TMB nanowires *via* a slow evaporation process wherein 1,3,5-TMB was added daily to maintain the concentration of C_{60} to be slightly lower than its saturation level and thus to prevent its precipitation in the solution.[31] The reactor was shaken several times a day to keep the wall of the reactor wet. A hard paper card held by a metal foldback clip was placed vertically to accelerate the process. The crystals grew both on the surface of the reactor and the paper card. It was found that the diameter of nanowires collected from the wall of the reactor varied from 350 nm to 750 nm. Y-shaped cross section which is the common morphology of C_{60}/1,2,4-TMB nanowires, however, was not observed in C_{60}/1,3,5-TMB nanowires. The diameters of the nanowires

collected from the paper card varied from 150 nm to 2 μm with a wider diameter distribution than those from the reactor wall.

2.2 Liquid-liquid interfacial precipitation (LLIP) method

Miyazawa *et al.* succeeded in preparing C_{60} nanowires by using a liquid-liquid interfacial precipitation (LLIP) method, with toluene or m-xylene (meta-xylene, or 1,3-dimethylbenzene) as solvent and isopropyl alcohol (IPA) or tert-butyl alcohol (TBA) as the precipitation agent.[11,22,32,33] The procedure of preparing C_{60} nanowires by LLIP method in toluene and IPA system was carried out as follow: A toluene solution of C_{60} (purity of 99.5%) with a concentration of 0.3 mass% C_{60} was prepared and poured into a glass bottle and then IPA was gently added on top of the solution to form a liquid-liquid interface. The bottle was sealed with an aluminium foil and kept undisturbed at room temperature until the C_{60} needle-like crystals grew out. Beakers of 100 mL volume were also used instead of the glass bottles to obtain a large quantity of C_{60} needle-like crystals. The C_{60} nanowires with thicknesses of about 10 nm, diameters of about 250 nm and a length-to-diameter ratio of up to 4000 were found out to be single crystalline and composed of thin slabs (Figure 4).[22]

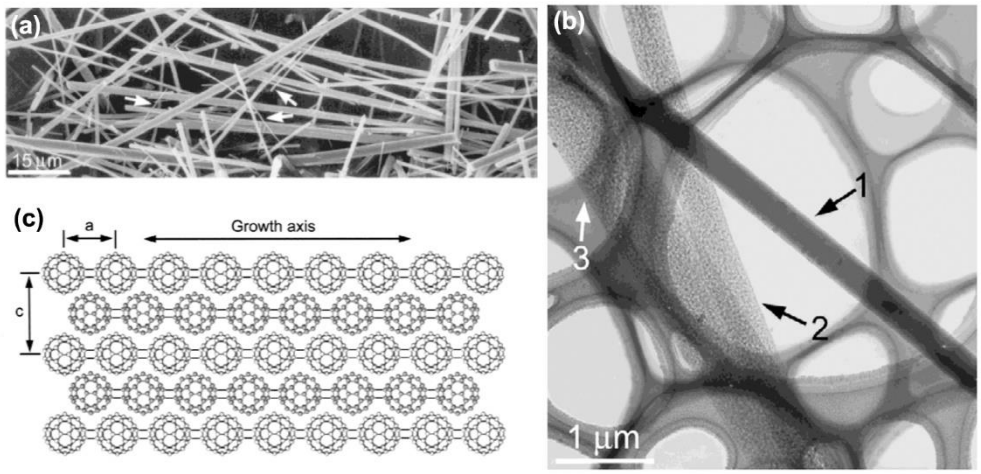

Figure 4. (a) SEM micrographs of the needle-like C_{60} nanowires in a beaker by the LLIP method. (b) TEM (200 kV) image of the C_{60} nanowires with different diameters. (c) A body-centered tetragonal (bct) model of C_{60} nanowire polymerized via "2 + 2" cycloaddition.[22]

Several strategies to modify the LLIP method were employed for the synthesis of C_{60} nanowires. In order to study the dependence of C_{60} nanowire growth on the two-solvent system, various solvents such as toluene, dichloromethane, hexane and their combinations were investigated. In the LLIP method, there is an interfacial pressure between a good solvent solution of C_{60} and a poor solvent of C_{60} which provides additional energy required for the polymerization of fullerene C_{60} molecules and thus enhances the polymerization. The interfacial pressure occurs due to: (i) pressure difference at the liquid-liquid interface caused by the different viscosities of the two liquids and (ii) Laplace pressure because of the interfacial tension between the liquids.[34] Therefore, increasing the difference of C_{60}

solubilities in the two solvents will improve the interfacial pressure, and consequently, will probably alter the morphology and structure of the resulting fullerene nanostructures. To prove this assumption, Sathish and Miyazawa prepared C_{60} nanowires using LLIP method in the carbon disulfide (CS_2) and IPA system instead of the commonly used toluene and IPA system and first obtained partially polymerized C_{60} nanowires. IPA (4 mL) was slowly added into the C_{60}-saturated CS_2 solution (1 mL) in a 50 mL glass bottle at a temperature of 5 °C using ice bath. The mixture was stored at 5 °C in an incubator with transparent plastic window for 24 h at ambient pressure (1 atm) to grow C_{60} nanowires. The diameter of the obtained fullerene nanowires ranged between 300 nm to 1 μm and their length was several tens of micrometres. They observed the fullerene polymerization at the liquid-liquid interface without any external pressure or photo-irradiation and confirmed that the high solubility of fullerene in CS_2 which markedly increased the liquid-liquid interfacial pressure was sufficient for the polymerization of nanowires.[25]

Miyazawa and Hotta also investigated the effects of the solvent ratio of the two liquids and water content on the growth of C_{60} nanowires in the toluene and IPA system using LLIP method.[24] A series of experiments using various solvent volume ratios of toluene to IPA between 1:7 and 7:1 was carried out. The growth of C_{60} nanowires was found to be enormously affected by the solvent ratio, and the nanowires grew longer above a critical diameter, which increased with the increase of the volume ratio of toluene to IPA. The best volume ratio of toluene to IPA showed was found to be 1:1 (Figure 5). Addition of a small amount of water into the C_{60}/toluene/IPA system was observed to promote the growth of C_{60} nanowires. In order to confirm this catalytic effect of water, experiments were performed by use of C_{60}-saturated toluene solution and a mixture of IPA and H_2O (no more than 2.5 mass % H_2O) with a ratio of 1:1. They found that the length of the C_{60} nanowires increased with the addition of water, while the diameter of the nanowires remained nearly the same, thereby providing a pathway to control the length-to-diameter ratio of C_{60} nanowires. To eliminate the effect of impurities of water contained in the C_{60}/toluene/IPA system, they also compared the effect of D_2O to water on the axial growth of the C_{60} nanowires. The addition of D_2O promoted the axial growth of C_{60} nanowires, but the effect was found to be a little weaker than that of H_2O possibly owing to the deuterium isotope effect.

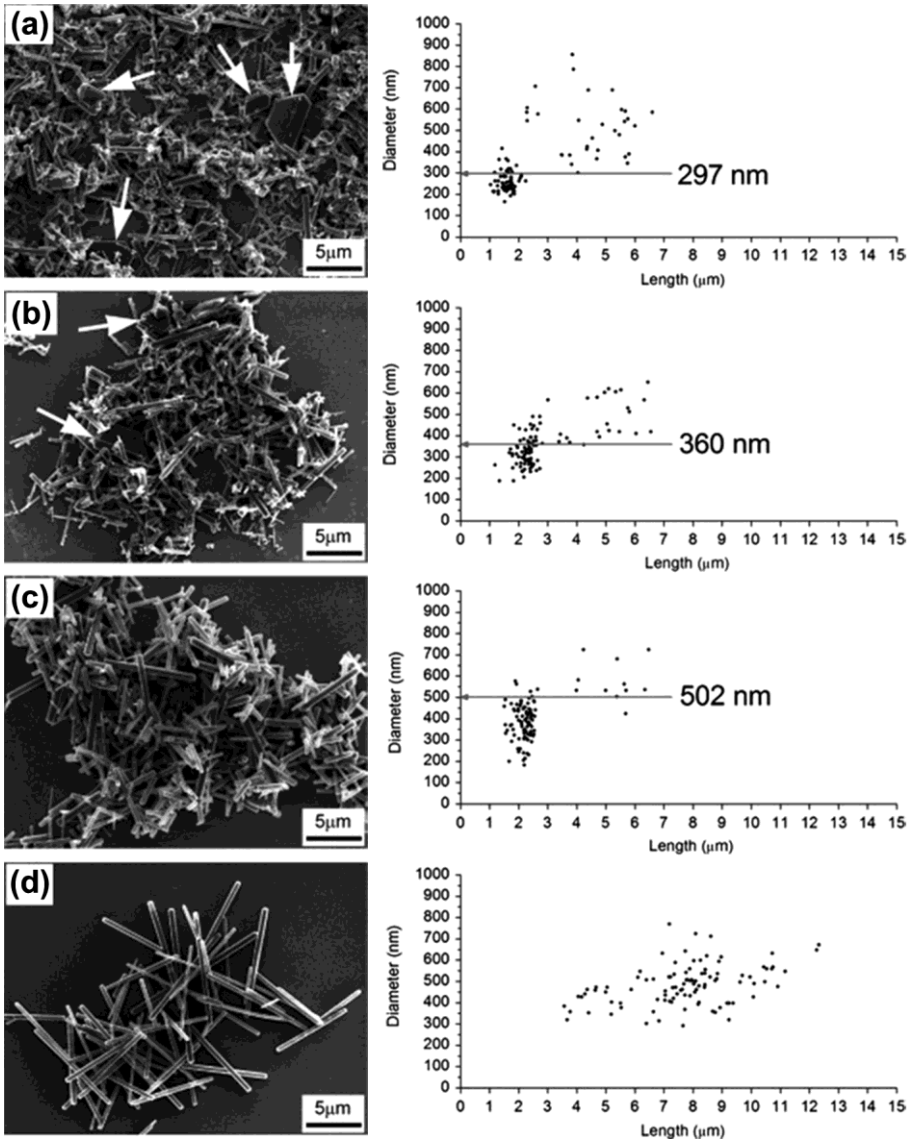

Figure 5. SEM micrographs (left) and the relationship between length and diameter (right) of the C_{60} nanowires formed at different solvent volume ratios of toluene and IPA for the growth time of 24 h at 20°C. Toluene: IPA (v/v) = (a) 1:7, (b) 1:5, (c) 1:3 and (d) 1:1.[24]

Moreover, Miyazawa and co-workers studied the influence of the size of the reactor (glass bottle) and the volume of the solution on the growth of C_{60} nanowires. The volume ratio of toluene and IPA in the experiments was kept at 1:1. Five transparent glass bottles of different sizes with inner diameters of 10 mm, 12.5 mm, 18.0 mm, 27.0 mm and 36.5 mm were used. The volumes of solutions inside these bottles were 1.5 mL, 3.0 mL, 8.0 mL, 20.0 mL and 80 mL respectively. The average lengths and diameters of C_{60} nanowires increased with the reactor size and thus the solution volume, however, the distribution of both their lengths and their diameters became wider (Figure 6). The mean size of the C_{60} nanowires crystal nuclei was estimated to be 5.02 μm in length and 387 nm in diameter by analysing the dependence of the size of C_{60} nanowires on the solution volume. The average lengths, diameters and length-to-width ratios for the C_{60} nanowires asymptotically approach their upper limits with the increasing of the solution volume. [35]

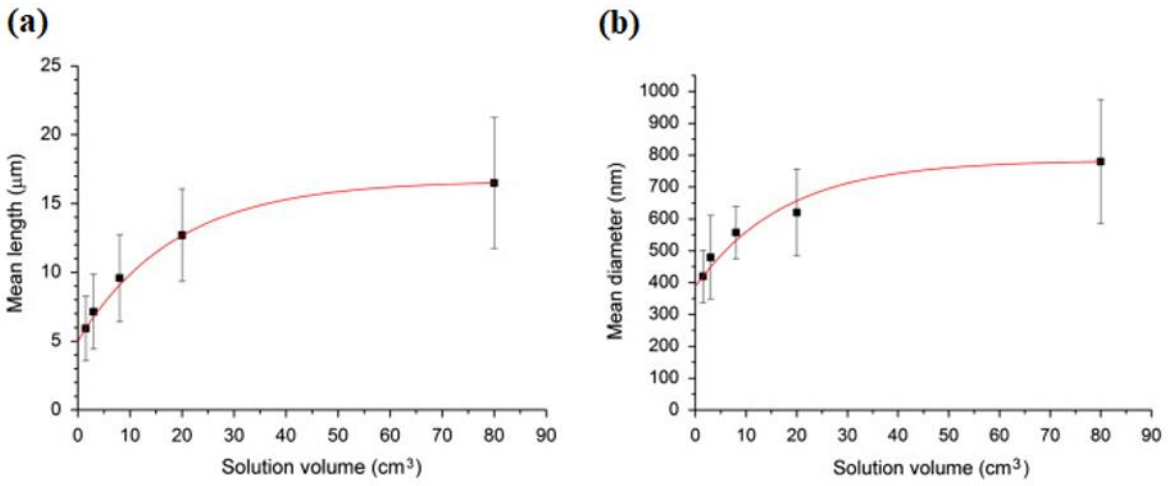

Figure 6. (a) Mean lengths of the C_{60} nanowires (y) plotted relative to the inner diameter of the bottle (x). The fitted curve equation is $y \sim -12 \exp(-x/18.7) + 17$. (b) Mean diameters of the C_{60} nanowires (y) plotted relative to the inner diameter of the bottle (x). The fitted curve equation is $y \sim -400 \exp(-x/17.6) + 800$.[35]

However, the glass bottle synthesis method has many drawbacks. Firstly, the process is quite slow, it usually takes more than one week to obtain stable C_{60} nanowires. Secondly, the size of the C_{60} nanowires for special applications cannot be controlled by this method. To solve these problems, microchannel reactors which have many advantages in the applications to gas-liquid, gas-gas, and liquid-liquid mixing have been employed in the preparation of C_{60} nanowires. Lee *et al.* used a silicon microchannel reactor of Y-type micromixer to synthesize C_{60} nanowires by LLIP method for the first time (Figure 7).[17] The reactor with two reactant delivery inlets (a, b) and two outlets (c, d) is illustrated in Figure 7(a). IPA and a solution of C_{60} in toluene were delivered in succession into inlet (a) and (b) of the reactor respectively using glass syringes connected to a syringe pump at a flow rate of 2000 μL/h. The growth of C_{60} nanowires was observed in the perpendicular direction of the reaction interface. The length and width of these C_{60} nanowires which were measured to be 200 μm and 2 μm showed better uniformity than those of the C_{60} nanowires synthesized by LLIP method using glass bottles, while their shapes were almost the same.

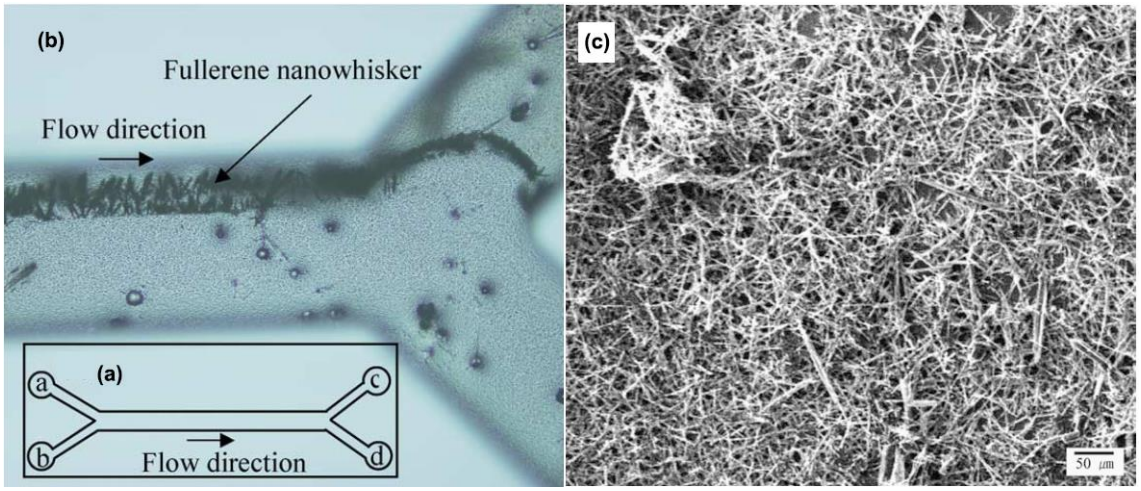

Figure 7. (a) Block diagram of the microchannel reactor. (b) Optical microscope picture of C_{60} nanowires synthesized at a liquid-liquid interface. (c) SEM micrograph of C_{60} nanowires obtained by the LLIP method in the microchannel reactor.[17]

It is known that C_{60} molecules are chemically polymerized under irradiation with laser light not only in solid but also in solutions.[26, 36-40] Thus, it is expected that the light can influence the growth of C_{60} nanowires. Photo-assisted polymerization of C_{60} has been reported in several literatures.[40-42] Tachibana synthesized C_{60} nanowires by a photo-assisted LLIP method at 21°C using weak room light (fluorescent light) as a light source and proved that the growth of C_{60} nanowires was promoted under illumination.[26] The longest nanowires with a diameter of about 250 nm reached a length of 1 mm and thus their length-to-width ratio reached ~ 4000. To examine the effect of light on the growth of C_{60} nanowires, the experiments were operated under four kinds of illumination conditions as shown in Table 1. They concluded that illumination contributed to both the nucleation and the growth of C_{60} nanowires, and that the characteristics of the illumination light, including intensity, wavelength and polarity of the light would affect the growth of C_{60} nanowires and thus the optimum illumination condition could lead to longer nanowires with faster growth rate (Figure 8).

Kato and Miyazawa investigated the photo-polymerization of C_{60} nanowires by using the Raman laser beam with a wavelength of 532 nm at various exposure conditions of the power density and the exposure time by using a Raman spectrometer in air at room temperature. It was found that an energy dose larger than about 1520 J/mm^2 was necessary for the laser beam of 532 nm wavelength to obtain the photo-polymerized C_{60} nanowires.[43]

Table 1. Four kinds of illumination conditions for the growth of C_{60} nanowires, and the total numbers and average lengths of as-prepared C_{60} nanowires within areas of 0.6 mm^2 on the glass substrates.[26]

Reactor	Illumination conditions		Grown C_{60} nanowires	
no.	Nucleation period	Growth period	Total number	Average length (μm)
1	Dark	Dark	129	13
2	Illumination	Dark	182	10

3	Dark	Illumination	115	98
4	Illumination	Illumination	233	232

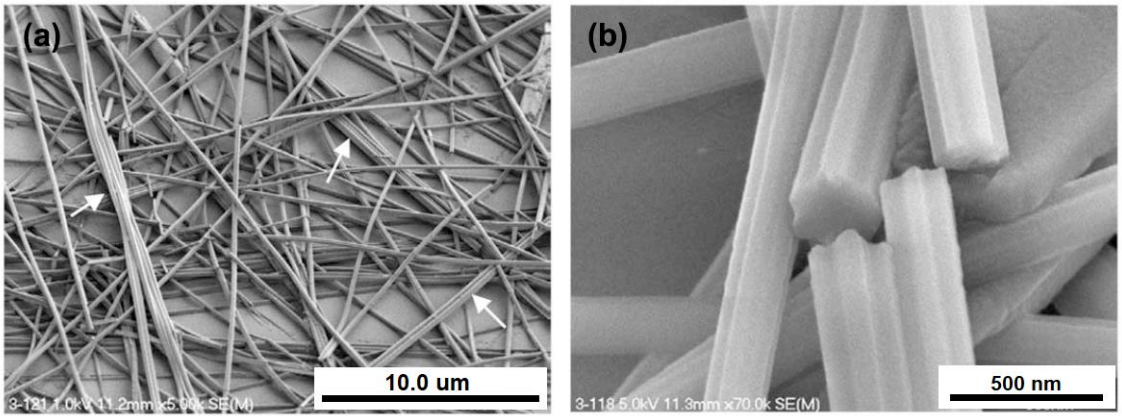

Figure 8. SEM images of C_{60} nanowires grown by LLIP method under illumination with fluorescent light at 21 ℃. (a) Bundled C_{60} nanowires (~5000). (b) Cross sections of C_{60} nanowires (~7000) showing star-like shapes with six-fold symmetry.[26]

LLIP method can be used for the synthesis of fullerene nanowires with multiple components. Miyazawa *et al.* have prepared C_{60}-C_{70} two-component fullerene nanowires by LLIP using m-xylene or pyridine as the solvent for C_{60}-C_{70} mixture and IPA.[44] Konno *et al.* have synthesized C_{60}-C_{70} nanowires using various ratios of C_{70} to C_{60}. The composition of the solutions ranged from 12.4 mass% C_{70} to 73.4 mass% C_{70}. The solid solubility limit of C_{70} in the matrix of C_{60} was estimated to be 13.7 mass%.[45]

Takeya *et al.* have prepared superconducting potassium (K)-doped C_{60} nanowires by the absorption of potassium to C_{60} nanowires obtained by LLIP method. C_{60} nanowires with overall diameters of 540 nm and lengths of 4.43 μm were filtrated and dried up in air. 10 mg of the C_{60} nanowires and 1.8 mg of potassium with a resulting molar ratio of K/C_{60} = 3.3 were mixed in a quartz tube (inner diameter of 5 mm) which was then sealed at 3×10^{-3} Pa. The mixture was heated at 200°C for 1-36 h in an electric oven to obtain K-doped C_{60} nanowires. The as-prepared K-doped C_{60} nanowires were shown to display superconductivity at 17 K.[46]

The LLIP-based methods are more suitable for quick and large-scale preparation for C_{60} nanowires than evaporation method. However, the uniformity of the C_{60} crystals obtained by LLIP method still remains a problem. Long and thin C_{60} nanowires, short and thick C60 nanorods, as well as some C_{60} crystals with other shapes are all mixed together in the solution, and thus, better separation methods need to be sought.

3. Characterization of C_{60} nanowires

To get a more profound understanding of C_{60} nanowires and to explore their potential applications, the properties such as morphology, structure and chemical composition of C_{60} fullerene nanowires must be analyzed and understood. An important aspect of the characterization of C_{60} nanowires is to study their morphology, crystalline structure and the way of how C_{60} molecules in the nanowires get polymerized. Optical microscopy, transmission electron microscopy (TEM), scanning electron microscope (SEM), X-ray powder diffraction (XRD), Raman spectroscopy have all been used to characterize the structure of C_{60} nanowires. Other analytical techniques such as gas chromatography-mass spectrometry (GC-MS), Fourier transform infrared spectroscopy (FT-IR), high-performance liquid chromatography (HPLC), and thermal gravimetric analysis (TGA) method have also been employed to study the chemical composition of C_{60} nanowires. However, there are only a handful of reports on the study of the mechanical and electrical properties of C_{60} nanowires.

3.1 Nanowire morphology and structure

C_{60} nanowires are wire-like 1-D structure with a length up to a few millimetres and a length-to-width aspect ratio as large as 4000. Due to the small size of C_{60} nanowires, optical microscopy, high-resolution electron microscopic techniques such as SEM and TEM, and atomic force microscopy (AFM) are employed to observe the morphology and structure of these nanowires, and these will be discussed in detail below.

3.1.1 Microscopy techniques

Wang *et al.* examined the morphology of C_{60} nanowires that were prepared by evaporation of a solution of C_{60} in m-xylene on silicon substrate by using SEM and AFM. AFM results indicated that the C_{60} nanowires had a rectangular cross section, the widths of the nanowires with different sizes were larger than their thicknesses, and the average thickness-to-width ratio was estimated to be ~0.45. The crystal structure of these C_{60} nanowires was also studied by TEM diffraction data analysed using Fast Fourier Transform (FFT) patterns. Both the high-resolution TEM (HRTEM) and FFT images showed that the C_{60} nanowires were single crystalline with a face-centered cubic (fcc) structure.[28]

Geng *et al.* utilized HRTEM to investigate the crystalline structure of the C_{60} nanowires.[10] The selected area electron diffraction (SAED) patterns and the ordered lattice images were obtained by controlling the beam brightness since the specimen was found to be electron beam sensitive. The HRTEM images (Figure 9 (a) and (b)) of the C_{60} crystal lattices viewed on the projections of [010] and [100] and the SAED patterns (Figure 9 (c), (d) and (e)) recorded down the [001], [010], and [100] directions revealed that the crystal structure of these C_{60} nanowires was orthorhombic, with the unit cell dimensions of a = 10.2 Å, b = 20.5 Å, and c = 25.6 Å.

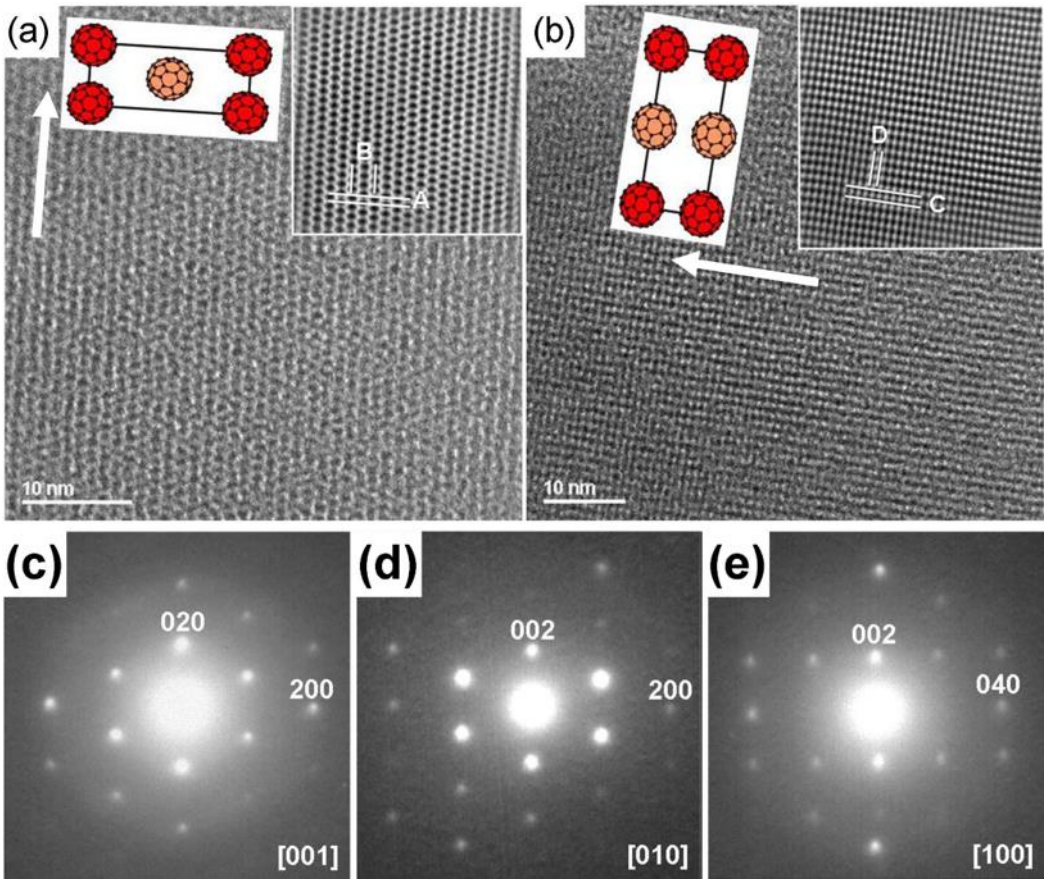

Figure 9. TEM image of the C_{60} nanowires. (a, b) HRTEM images of the nanowires along the [010] and [100] directions, respectively. The insets in (a) and (b) are computer-created corresponding images after removing the background noise (right corners) and the corresponding projections of the structure. The *d*-spacings are indicated by using the A (100), B (001), C (002), and D (020) planes. The arrows indicate the growth directions of the C_{60} nanowires. (c, d and e) SAED patterns viewed along the [001], [010], and [100] zone axis of the orthorhombic unit cell, respectively.[10]

In their later research, similar analytical techniques were employed for the characterization of the C_{60} nanowires. 1D C_{60} nanocrystals with three nanobelts along the growth direction were also observed. The length of the C_{60} nanowires was typically ~200-600 μm, and the length-to-width aspect ratio was estimated as large as ~3000. These nanowires possessed a prism-like central core and three nanobelts joined along the growth direction to give an overall Y-shaped cross section as shown in Figure 10. By applying HRTEM and SAED on the C_{60} nanowires, the crystal structure was determined to be orthorhombic, the same as that of the two-wing nanowires.[30]

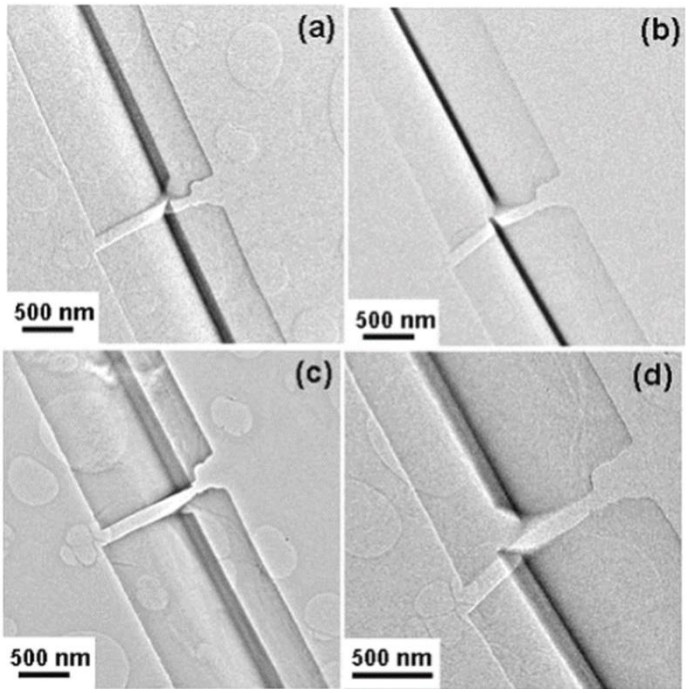

Figure 10. TEM images of a thick but broken nanowire recorded with varied tilting angles of the sample grid (a-d) to show the overall morphology and the three nanobelt-like wings.[30]

3.1.2 X-ray powder diffraction (XRD)

Minato and Miyazawa characterized the structure of C_{60} nanowires prepared by the LLIP method in a C_{60}-saturated m-xylene and IPA system.[33] Morphological observations were performed using an ordinary optical microscope and a TEM. The length of the nanowires reached several tens of micrometres. Both TEM and XRD measurements showed that the C_{60} nanowires had a hexagonal structure with lattice constants of a = 2.407 nm and c = 1.018 nm which was different from that of the pristine C_{60} (a = 1.415 nm). The dependence of XRD pattern on time was also studied to investigate the change in structure of C_{60} nanowires during the drying process. It was found that within 69 min of the evaporation of solvent molecules in air, the structure of the C_{60} nanowires transformed from a solvated structure into a *fcc* structure with a lattice constant of a = 1.420 nm which was close to the value of the pristine C_{60} (Figure 11).

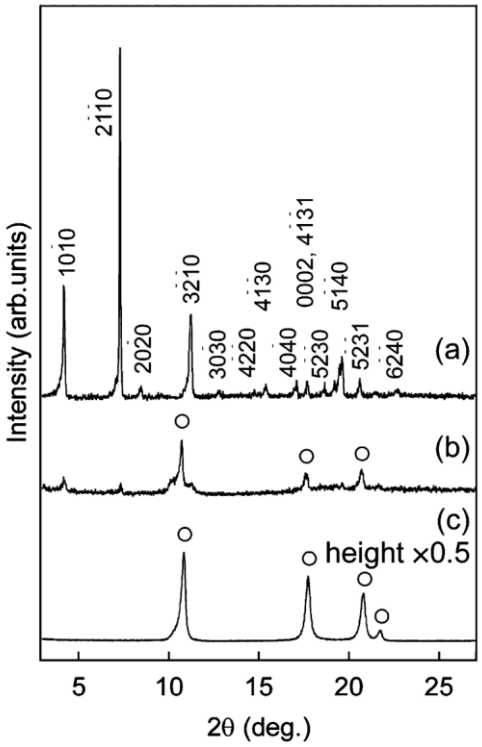

Figure 11. XRD patterns of C_{60} nanowires made in C_{60}/m-xylene/IPA system after (a) 29 min, and (b) 69 min, for sampling from the glass bottle. (c) XRD pattern of pristine C_{60}. The peaks indicated by open circles correspond to the *fcc* structure of C_{60}.[33]

Konno *et al.* synthesized the two-component C_{60}-C_{70} fullerene nanowires by LLIP method using various ratios of C_{70} to C_{60}.[45] XRD patterns of both C_{60} nanowires and C_{60}-C_{70} nanowires (the latter was made by using a solution of C_{60} and C_{70} with a concentration of 24 mass% C_{70}) are shown in Figure 12. Peaks corresponding to an *fcc* phase and a triclinic (*tr*) phase were observed in the C_{60} nanowires. The *tr* phase was assumed to be formed by distortion of the *fcc* phase and the calculated lattice constant of the *fcc* phase was a = 1.4227 ± 0.005 nm. Peaks corresponding to an *fcc* phase and a *tr* phase as well as a rhombohedral (*rh*) phase were observed in C_{60}-C_{70} nanowires. The calculated lattice constant of the *fcc* phase was a =1.4337 ± 0.011 nm. It was suggested that the addition of C_{70} molecules might be the cause for the partial polymerization of C_{60} molecules.

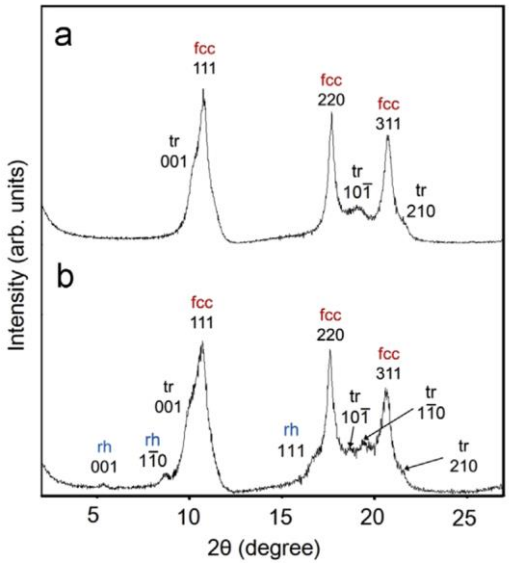

Figure 12. XRD patterns of (a) C_{60} nanowires, and (b) the C_{60}-C_{70} two-component nanowires, prepared using a mother solution with a composition of C_{60}-24 mass% C_{70}.[45]

Sathish and Miyazawa prepared C_{60} nanowires by LLIP method in a CS_2 and IPA system.[25] The field emission scanning electron microscopy (FE-SEM) image of C_{60} nanowires showed that the diameter of the C_{60} nanowires was 300 nm to 1 μm and the length was several tens of micrometres. The XRD pattern of these C_{60} nanowires after 24 h of incubation was obtained using XRD with CuKα radiation (Figure 13) and then compared with that of pristine C_{60}. Peaks corresponding to an *fcc* phase were observed in C_{60} nanowires, the lattice constant was determined to be a = 1.416 ± 0.003 nm. Peaks corresponding to a *tr* phase with lattice constants of a = 1.033(2) nm, b = 0.971(1) nm, c = 1.127(3) nm, α = 53.7°, β = 52.3°, γ = 58.3° were also observed, which indicated the partial polymerization of C_{60} molecules in the C_{60} nanowires. While only a slightly polymerized phase of C_{60} molecules was observed in nanowires prepared in a toluene and IPA system or a benzene and IPA system as reported, there was a more obvious polymerized phase in C_{60} nanowires prepared in the CS_2 and IPA system. They drew a conclusion that the partial polymerization of C_{60} molecules in the nanowires might be taking place at the C_{60}-saturated CS_2 and IPA interface due to the relatively high interfacial forces caused by the large difference in solubilities of C_{60} in CS_2 and IPA.

It is noted that a range of different crystal structures was found in fullerene nanowires, which was believed to be a result from different growth methods or use of different solvents in growths. Table 2 is a summary of the crystal structures of fullerene nanowires reported in literature.

Table 2. Crystal structures of fullerene nanowires made by different growth methods.

Main Composition	Growth Method	Solvent	Structure	Reference
C_{60}	Evaporation	m-xylene	Face-centred cubic (fcc)	28
C_{60}	Evaporation	1,2,4-TMB	Orthorhombic	10
C_{60}	Evaporation	1,2,5-TMB	Orthorhombic	30
C_{60}	LLIP	m-xylene and IPA	Hexagonal, fcc	33
C_{60}	LLIP	toluene and IPA	fcc, triclinic (tr)	45
C_{60} and C_{70}	LLIP	toluene and IPA	fcc, tr, Rhombohedral (rh)	45
C_{60}	LLIP	CS2 and IPA	Fcc, tr	25

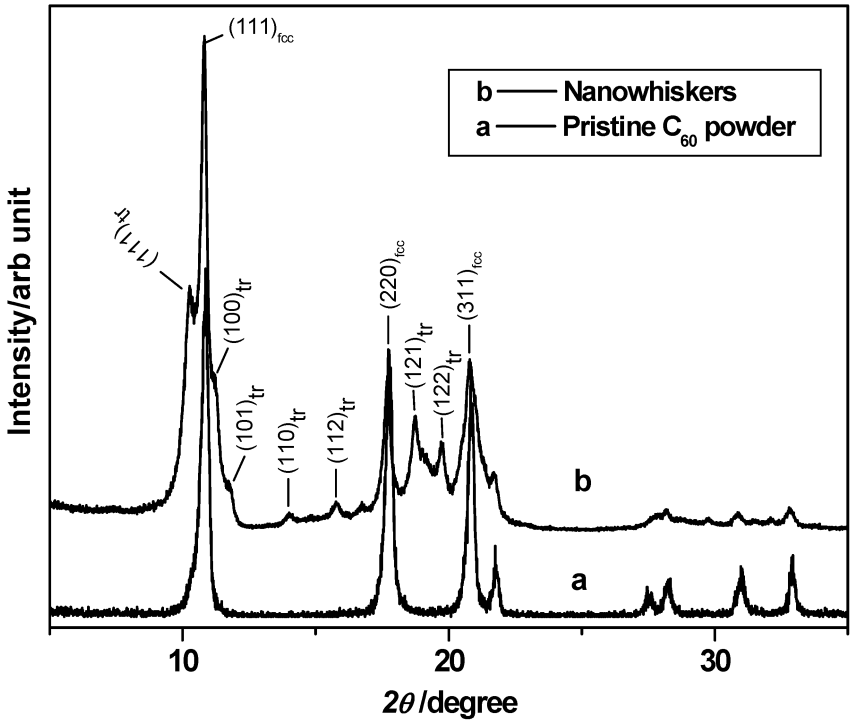

Figure 13. XRD patterns of (a) pristine C_{60} powder, and (b) C_{60} nanowires obtained by LLIP method in the C_{60}/CS_2/IPA system.[25]

3.1.3 Raman spectroscopy

Raman spectroscopy is a useful technique for identification of a wide range of substances and a powerful tool to analyze C_{60},[28, 39, 47-50] including studies of the polymerization of C_{60} molecules in C_{60} nanowires. Tachibana *et al*. examined the intermolecular bonding in C_{60} nanowires prepared by LLIP method using Raman spectroscopy at 294 K in air. As shown in Figure 14, the peak intensity at 1468 cm^{-1} corresponding to $A_g(2)$ mode reduced significantly while that of 1458 cm^{-1} increased with

increasing irradiation time, which indicated that the polymerization of C_{60} nanowires only occurred under the laser irradiation, while no photochemical polymer was found in pristine C_{60} nanowires. They concluded that C_{60} molecules in the pristine nanowires were bonded by only weak van der Waals forces.[26]

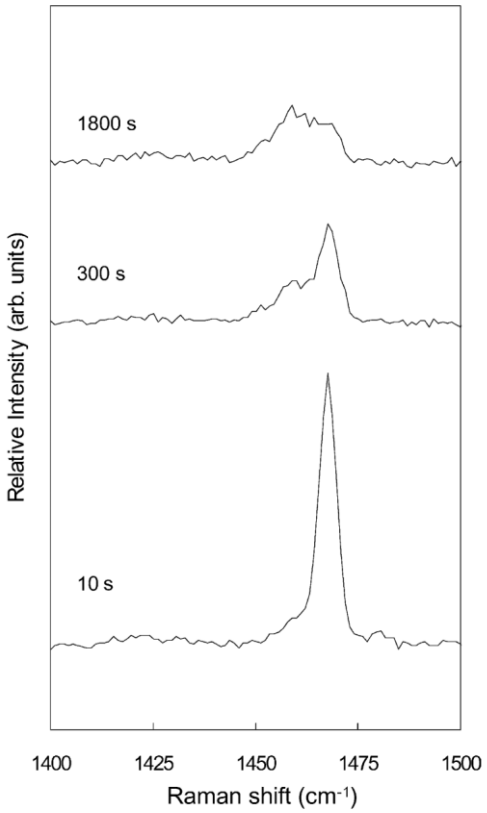

Figure 14. The time evolution of Raman spectra of C_{60} nanowires near the $A_g(2)$ pentagonal pinch mode at 294 K in air, irradiated by a 532 nm laser with a low power density (~100 mW/mm^2). The irradiation time is indicated to the left in figure.[26]

Geng *et al.* investigated the isolated C_{60} molecules within the nanowires with a V-shaped cross section by comparing the laser Raman spectra of C_{60} nanowires with raw C_{60} powder. As shown in Figure 15, peaks at 494 and 1467 cm^{-1} corresponding to A_g mode and a number of peaks corresponding to H_g mode at 273, 773, 1122, 1420, 1569 cm^{-1} were observed. It was concluded that no polymerization occurred and C_{60} in the nanowires were pristine C_{60} molecules as the polymerization would cause a shift of the peak from 1468 cm^{-1} to 1458 cm^{-1} which is the signature of C_{60} in the photo-transformed or polymeric state. Following a heat treatment in argon to 900°C under a temperature increase rate of 5°C/min, these nanowires were transformed into carbon nanofibers. Laser Raman test showed that the original crystalline structure was lost and a new disordered carbon microstructure was formed, which was in accordance with the HRTEM result.[10]

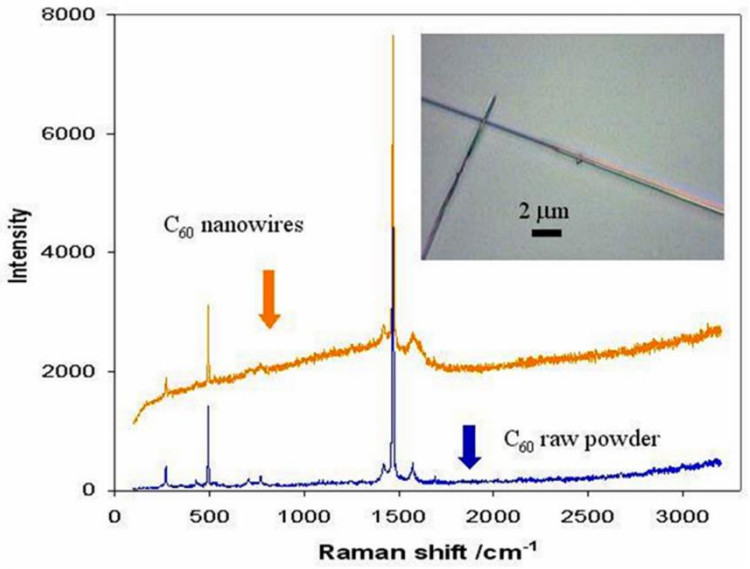

Figure 15. Laser Raman spectroscopy of the C_{60} nanowires (obtained by the evaporation of solutions of C_{60} powder in 1,2,4-TMB) and the raw C_{60} powder.[10]

Sathish *et al.* confirmed the polymerization of C_{60} molecules in the C_{60} nanowires synthesized by LLIP method in a CS_2 and IPA system by Raman spectroscopy (Figure 16), which was consistent with the XRD observation as mentioned above. Since the interfacial forces generated at the liquid-liquid interface may not be strong enough to completely polymerize the C_{60} molecules, a partial polymerization occurred during the preparation itself due to the interfacial forces, and the polymerization was further enhanced by the laser light used for Raman spectroscopic measurements.[25]

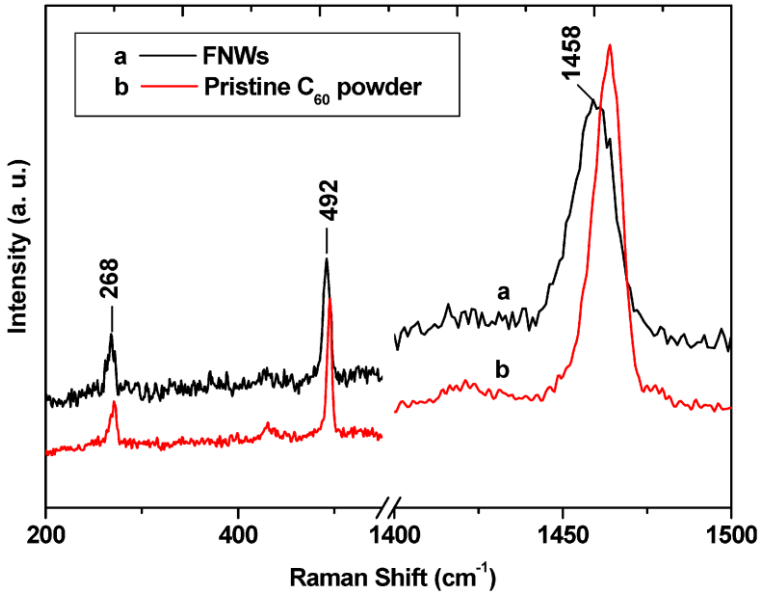

Figure 16. Laser Raman spectroscopy of (a) the C_{60} nanowires obtained by the LLIP method in the C_{60}/CS_2/IPA system and (b) the pristine C_{60} powder.[25]

Calamba *et al.* prepared a hybrid material named FW/PANI hybrid by the addition of polyaniline emeraldine base dissolved in N-methyl-2-pyrrolidone (PANI/NMP) on fullerene C_{60} nanowires using direct-mixing technique.[51] The vibrational frequencies of the hybrid were measured using a microscopic Raman spectrophotometer. A series of characteristic peaks of PANI in regions of 1150-1250 cm^{-1}, 1350-1450 cm^{-1} and 1550-1650 cm^{-1} was found. A sharp peak at 1467 cm^{-1} corresponding to A_g mode of C_{60} was also observed, which indicated that C_{60} molecules in the FW/PANI hybrid were bonded by van der Waals forces.

3.2 Chemical composition

Polymerized C_{60} nanowires are composed almost entirely of carbon. A small number of solvent molecules may exist in the nanowire structure. Analytical techniques including GC-MS, FT-IR, HPLC, Raman spectroscopy and TGA have been employed to study the chemical composition of C_{60} nanowires. HPLC and Raman spectroscopy can also be used to calculate the composition ratio in the two-component C_{60}-C_{70} nanowires.

3.2.1 Gas chromatography and mass spectrometry (GC-MS)

GC-MS is an analytical method that combines the features of gas-chromatography and mass spectrometry to identify different substances within a test sample. Watanabe *et al.* analyzed the residual solvent molecules in C_{60} nanowires obtained by LLIP method in a toluene/IPA solvent system by GC-MS. Figure 17 is the GC spectra of C_{60} nanowires with drying treatment in vacuum for 5 minutes, the peak at 0.925 min is for CO_2, N_2 and water introduced to the system due to sample injection or absorbed on the nanowire surface. Figure 17 (b) and 17 (c) are the mass spectra corresponding to the peak of 2.33 min and 1.067 min in Figure 17 (a) respectively. The peaks at 91 and 92 Da in Figure 17 (b) proved the existence of toluene molecules, while the peaks of 43 and 45 Da in Figure 17 (c) showed the fragments of IPA molecules. The amount of toluene molecules was more abundantly contained in C_{60} nanowires than IPA, with a quantity of residual toluene of about 7%mass, this is because C_{60} molecules are well dissolved in non-polar solvents but poorly dissolved in polar solvents.[52]

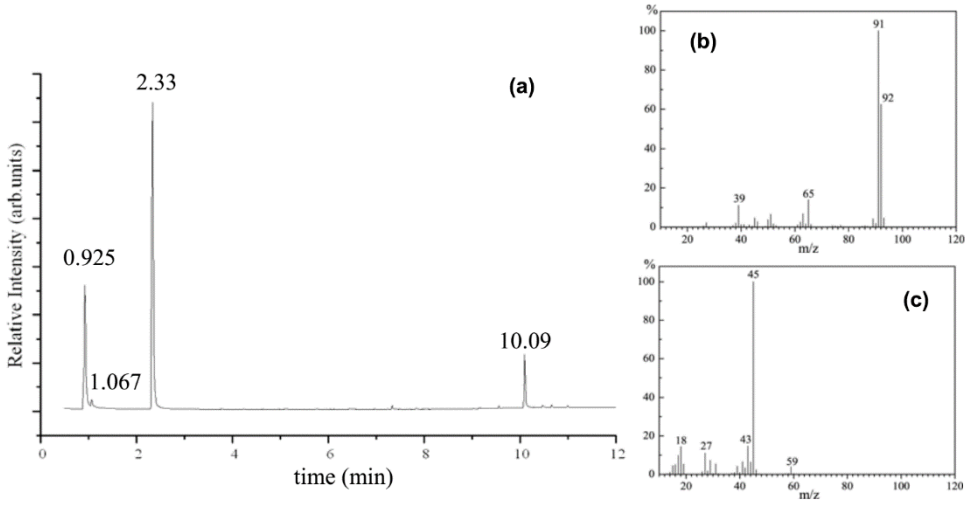

Figure 17. GC-MS analysis of the chemical composition of the C_{60} nanowires obtained by LLIP method in the C_{60}/toluene/IPA system. (a) GC spectra of as-prepared C_{60} nanowires after drying in vacuum for 5 min. (b) Mass spectra for the peak of 2.33 min in (a). (c) Mass spectra for the peak of 1.067 min in (a).[52]

Using GC-MS, Geng *et al.* identified the guest species in the C_{60} nanowires which was approved to be the 1,2,4-TMB molecules employed as solvent for the crystal growth (Figure 18). They successfully identified three components including the remnants of the CCl_4 from the injection (the peak at 2.06 min) and two isomers of 1,2,4-TMB molecular (the peaks at 2.99 and 3.28 min). The mass spectra of the components isolated by GC indicated that the nanowires contained 1,2,4-TMB molecules within their crystal lattices, which was consistent with the structural analysis by HRTEM and the electron diffraction patterns.[10, 53]

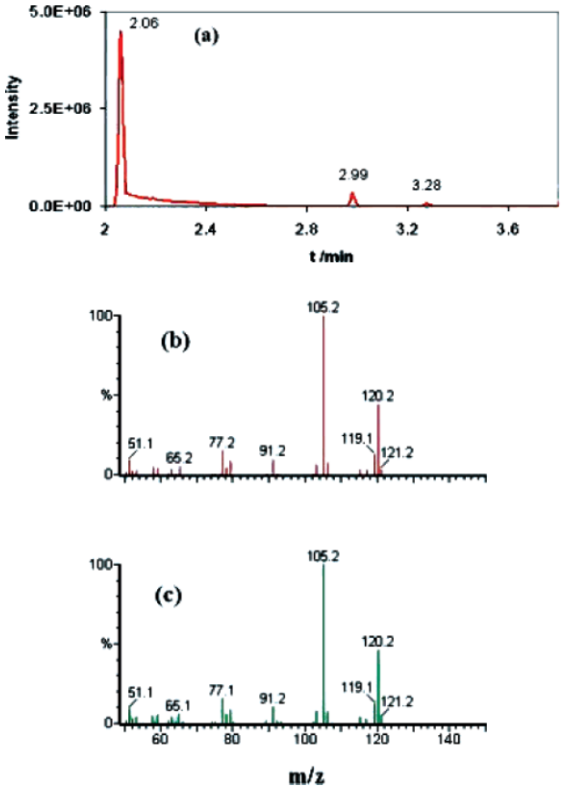

Figure 18. GC-MS analysis result for the chemical composition of the C_{60} nanowires obtained by evaporation of C_{60} solution in 1,2,4-TMB. (a) GC result from the dissolved sample in CCl_4. (b and c) Mass spectra of the components isolated by GC and labelled by the peaks 2.99 and 3.28 in (a), respectively.[10]

3.2.2 Fourier transform infrared spectroscopy (FT-IR)

FT-IR can be used to obtain an infrared spectrum of absorption or emission of a solid, liquid or gas. Yao *et al.* carried out IR analysis on C_{60} nanowires grown from m-dichlorobenzene, m-dibromobenzene, and m-diiodobenzene solutions by evaporation method. IR spectra (Figure 19) showed the existence of signals from the solvents used (marked with rings) in addition to the unpolymerized C_{60} signals, which indicated that m-type solvents remained in the structure of C_{60} crystals and the C_{60} molecules were pristine.[29]

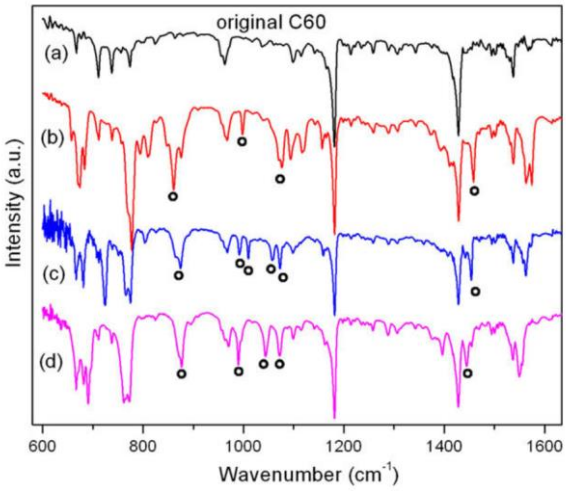

Figure 19. IR spectra of (a) original C_{60}, (b) C_{60} nanowires obtained from solutions in m-dichlorobenzene, (c) m-dibromobenzene, and (d) m-diiodobenzene. Solvent bands are marked with rings.[29]

Miyazawa and co-workers performed FT-IR measurement on fine needle-like C_{60} crystals formed through LLIP method using an interface of concentrated C_{60} solution in toluene and IPA.[22] In the FT-IR spectrum shown in Figure 20, the characteristic peaks of pristine C_{60} at 527, 577, 1182, 1428 cm^{-1} confirm that the nanowires were composed of C_{60} molecules. The absorption peaks at 556, 604, 725, 1073, and 1636 cm^{-1} were similar to those of the C_{60} polymer with approximately 50 % orthorhombic phase + approximately 50 % tetragonal phase prepared by compressing C_{60} powder under 1.1 GPa at 600°C.[22, 54]

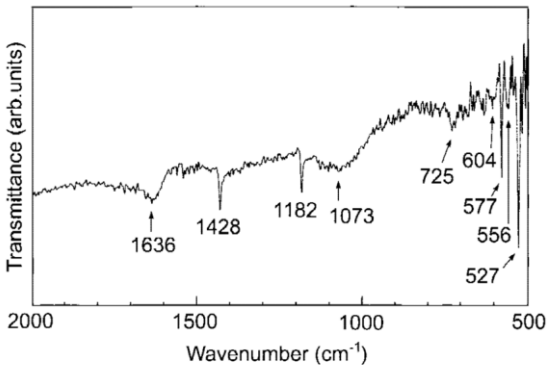

Figure 20. FT-IR spectrum of the C_{60} nanowires obtained by LLIP method in the C_{60}/toluene /IPA system.[22]

Minato *et al.* examined the pristine C_{60} powder, the nanowires grown in the C_{60}-saturated m-xylene and IPA system, and m-xylene respectively by using FT-IR and compared their spectra obtained. Peaks at 527, 575, 1182, 1428 cm^{-1} in Figure 21 (a) and Figure 21 (b) indicate that the nanowires were composed of C_{60} molecules, while peaks at 690 and 767 cm^{-1} prove the existence of m-xylene molecules in the crystal structure.[33]

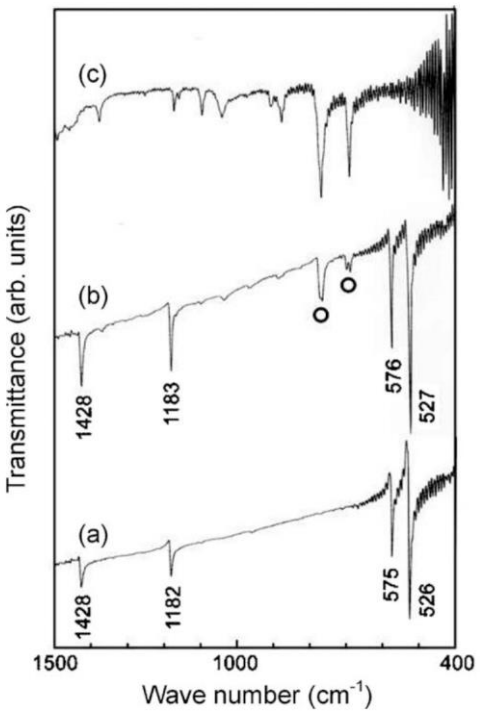

Figure 21. FT-IR spectra of (a) pristine C_{60}, (b) C_{60} nanowires obtained by LLIP method in the C_{60}/m-xylene/IPA system, and (c) m-xylene.[33]

3.2.3 High-performance liquid chromatography (HPLC)

In an aforementioned research by Konno and co-workers, C_{60}-C_{70} nanowires were prepared using a C_{60}-C_{70} two-component solution under different mixing ratios of C_{60} and C_{70}-saturated solutions in toluene. The chemical compositions of both the supernatant solutions and the precipitates were determined by HPLC (Figure 22, a and b). Figure 22 (a) indicates the solid solubility of 12.4 mass% of C_{70} in the matrix phase of C_{60}, and the solid solubility of 26.6 mass% of C_{60} in the matrix phase of C_{70}. As shown in Figure 22 (a) and (b), C_{70} and C_{60} were unsaturated in the supernatant solutions for compositions at ranges of 0-12.4 mass% C_{70} and 73.4-100 mass% C_{70}, respectively. Both C_{60} and C_{70} were saturated in the supernatant solutions for compositions ranging from 12.4 mass% C_{70} to 73.4 mass% C_{70}.[45] They also performed HPLC measurements on individual thick needle-like C_{60}-C_{70} crystals. It was found that these crystals contained 11.1 ± 2.2 mass% C_{70} and up to 13.7 mass% C_{70}, while the mother solution contained 45.4 ± 4.1 mass% C_{70}. The solid solubility of C_{70} in the matrix phase of C_{60} was 13.7 mass%, which was close to the result of 12.4 mass% C_{70} in Figure 22 (a).

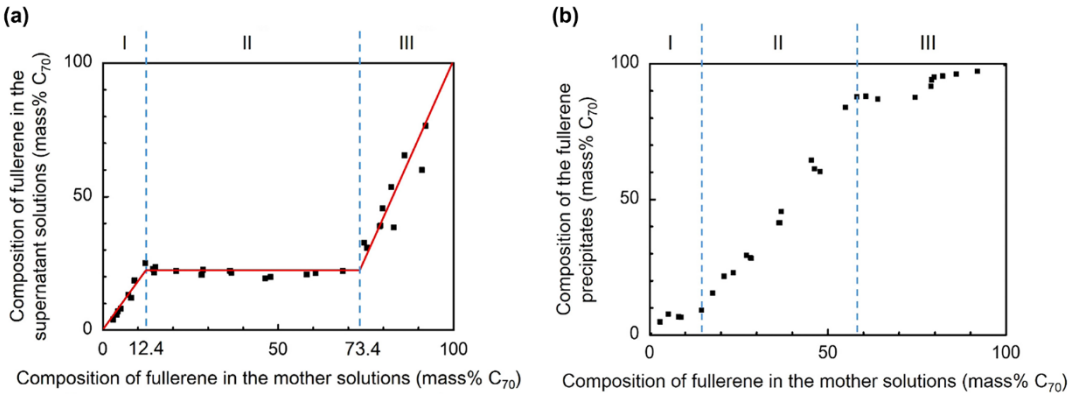

Figure 22. Chemical composition of (a) the supernatant solutions and (b) the precipitates determined by HPLC.[45]

3.2.4 Raman spectroscopy

Konno *et al.* measured the composition of C_{60}-C_{70} two-component nanowires by Raman spectroscopy and determined their composition by calculating the peak area ratios which have a linear relationship with the composition (mass% C_{70}). They compared the chemical composition of the C_{60}-C_{70} nanowires to that of the granular precipitates as determined by Raman spectroscopy (Figure 23) and found that when the composition of fullerene in the mother solution is 9 mass% C_{70}, the compositions in the granular precipitates and the C_{60}-C_{70} nanowires were nearly the same, but when it came to more than 18 mass% C_{70}, the composition of fullerene (mass% C_{70}) in the granular crystals is much higher than that in the C_{60}-C_{70} nanowires. They concluded that the granular precipitates abounded in C_{70} molecules when the composition in the mother solutions exceeded the solid solubility limit of C_{70} in the matrix phase of C_{60}.[45]

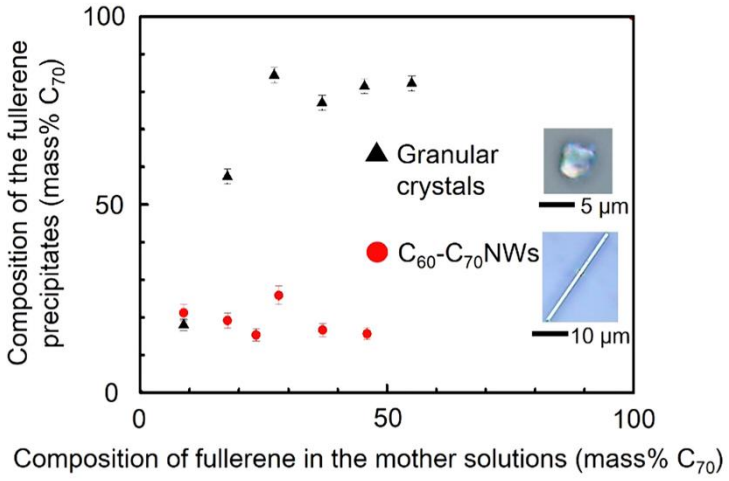

Figure 23. Chemical composition of the granular crystals and the C_{60}-C_{70} two-component nanowires determined by Raman spectroscopy.[45]

3.2.5 Thermal gravimetric analysis (TGA)

Miyazawa performed TGA on C_{60} nanowires prepared by LLIP method in the toluene and IPA system in vacuum at a rate of temperature increase of 10°C. Before TGA, C_{60} nanowires were dried up at room temperature in air. They found that the C_{60} nanowires began to decompose at a temperature higher than 550°C in vacuum. The decrease in the TGA curve with increasing temperature indicated the removal of solvent molecules contained in the nanowire structure.[55]

Geng *et al.* determined the ratio of the 1,2,4-TMB to C_{60} in C_{60} nanowires grown from a 1,2,4-TMB solution through direct evaporation method by TGA that was performed in an argon atmosphere (Figure 24). TGA were also performed on raw C_{60} powder for comparison. As shown in Figure 24, 1,2,4-TMB molecules were gradually removed from the material below the temperature of 644°C, and above that temperature, C_{60} began to sublimate. The TGA result also showed that there was a considerable amount of C_{60} that could not be sublimated but simply remained as residue at temperatures up to 900°C. It was estimated that the weight percentage of 1,2,4-TMB and C_{60} in the nanowires was ~14.7 wt % and ~85.3 wt %, respectively. Accordingly, the molar ratio of 1,2,4-TMB to C_{60} was ~1:1.[10]

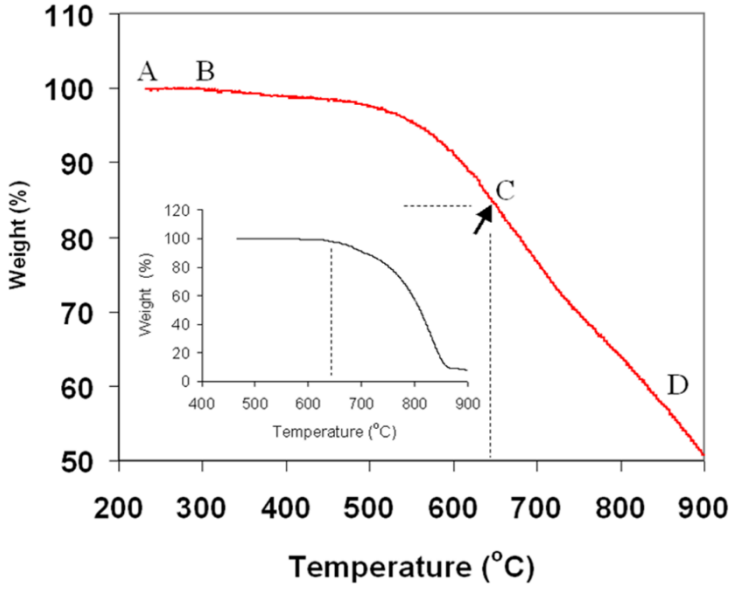

Figure 24. TGA analysis result of the C_{60} nanowires. The temperature increase rate is 5°C/min in argon. The inset shows the result from raw C_{60} powder with a high purity of 99.9%.[10]

3.3 Mechanical properties

Asaka *et al.* prepared C_{60} nanowires with a high length-to-width aspect ratio by LLIP method using C_{60}-saturated pyridine and IPA system and observed their compressive deformation.[56] The suspension of C_{60} nanowires was dropped onto a microgrid which was mounted on a specimen holder for a TEM equipped with an optical lever force measurement system. A microcantilever with a nanometre-sized silicon tip coated with a gold film fixed on another specimen holder was used to applied force to the tip of the C_{60} nanowire, as shown in Figure 25. The deformation of the C_{60} nanowires was observed in situ using a TV rate system with a time resolution of 17 ms. Variations in force applied to the C_{60} nanowires were measured by optical lever method during the deformation process. They found that a C_{60} nanowire with a diameter of 160 nm fractured in the middle at a strain of 0.08, and the Young's modulus of the nanowires with a diameter of 130 nm and 160 nm were determined to be 32 ± 6 GPa and 54 ± 3 GPa respectively, which were 60 % - 550 % higher than that of C_{60} bulk crystals. The high value of Young's modulus of the C_{60} nanowires might promise their applications on various flexible components of nanometre-sized composites.[56]

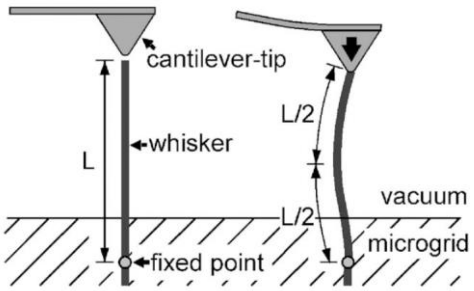

Figure 25. Compressive deformation of C_{60} nanowires by TEM equipped with functions of scanning probe microscopy.[56]

Larsson and co-worker developed an experimental bespoke silicon-based microelectromechanical system (MEMS) electrothermal 4-point bend tester to analyze the mechanical properties of thick C_{60} wires of 4 μm in diameter.[57] An individual C_{60} wire prepared by LLIP method using a C_{60}-saturated toluene and IPA system was placed between the anvils of the bend tester and observed under an optical microscope. A Young's modulus of only ~2 GPa is obtained with a C_{60} nanowire of through parameter extraction techniques. The value was much smaller than those of thin C_{60} nanowires of 130 nm and 160 nm in diameter in previous report,[56] which suggested an inverse proportionality relationship between the Young's modulus and the diameter of C_{60} 1D crystals. However, this technique is not suitable for the characterization of thin C_{60} nanowires with a diameter of less than 500 nm due to the high van der Waal's forces between the nanowires and the silicon surface of the anvil and platform of this device.

3.4 Conductivity

Miyazawa *et al.* measured the resistivity of C_{60} and C_{70} nanowires prepared by LLIP method in the m-xylene and IPA system using a micromanipulator equipped with a two-channel source/monitor unit.[44] It was found that the resistivity of C_{60} wire-like crystals rapidly decreased with the reduction in the diameter and heat treatment in vacuum helped to increase the electrical conductivity of these crystals. C_{70} wires were found to exhibit lower resistivity than C_{60} wires by a factor of about 10~100. C_{60} nanowires prepared using m-xylene as the solvent (with a resistivity range of 10^3-10^7 Ω·cm)[44] were observed to have better conductivity than C_{60} nanowires prepared using toluene as solvent (with a resistivity range of 10^8-10^{10} Ω·cm),[21] which was probably due to the difference in their crystal structures.

Larsson *et al.* reported four-point probe (4-PP) measurements on individual thick C_{60} wires and thin C_{60} nanowires prepared by LLIP method with diameters in the range 650 nm to 1.3 μm.[58] The C_{60} wires were attached to the pre-patterned thermally oxidised silicon substrates and the raised electrodes through focused ion beam (FIB)-assisted deposition of metal using a beam of Ga ions (Figure 26). The resistivity of a C_{60} nanowire with a diameter of 650 nm was measured to be 3 Ωcm. The low value of resistivity implied that C_{60} nanowires with diameters of submicrometre-scale can find potential applications in low-power organic electronic applications without the need for a protective inert atmosphere.[58]

Generally speaking, C_{60} nanowires are poor in electrical conductivity because of the gaps between C_{60} molecules in crystalline form. So the nanowires are insulator and in some cases, they could be semi-conductor. Polymerized C_{60} nanowires could have increased electrical conductivity because of the linkage of C_{60} molecules by guest molecules (solvent molecules) in the crystal structure, but more research work needs to be done in the future to confirm this view and to explore the use of the material in electrical field as well. The electrical conductivity of C_{60} nanowires is caused by the conducting overlapped π electrons in C_{60} nanowire structure. Shorter C_{60} intermolecular distances and more closed packed C_{60} nanocrystal structures lead to greater overlap of π electrons in C_{60} nanowires, and thus higher conductivity.[44, 59, 60]

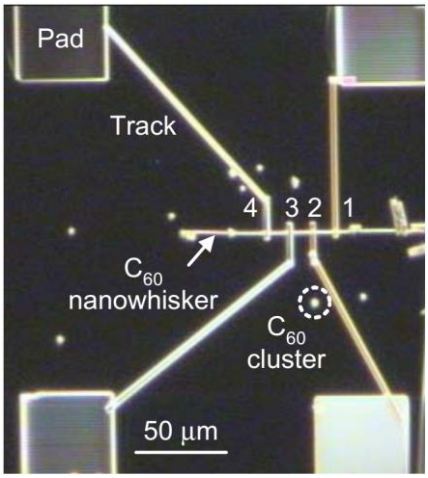

Figure 26. Microscope image of a single C_{60} nanowire with a diameter of 400 nm on a silicon platform with 4-PP FIB-deposited electrode.[58]

4. Mechanistic studies on growth

A good understanding of the growth mechanism of C_{60} nanowires is of great importance to their size control, large-scale preparation, and the exploration of their future applications in a wide range of fields. The mechanisms of C_{60} nanowires growth and their post-growth polymerization have been discussed in a few reports. However, these still need to be studied in more details for materials prepared under different experimental conditions.

Miyazawa *et al.* proposed a mechanism of the growth of C_{60} nanowires through LLIP method, which points that the crystal growth is driven by the high pressure between the liquid-liquid interface. The C_{60} molecules themselves are confined into a very thin space of interface, where the pressure can reach orders of GP, and thus the C_{60} molecules are two-dimensionally polymerized.[22] They found that the intermolecular distance in the C_{60} nanowires was shorter in the close-packed direction compared with that in pristine C_{60} crystals, thus indicating the strong bonding between C_{60} molecules and suggesting that the C_{60} nanowires were polymerized through "2 + 2" cycloaddition in the close-packed [110]c direction (Figure 4(c)).[22]

Tachibana *et al.* suggested that there are two stages during the formation of C_{60} nanowires using LLIP method. C_{60} molecules nucleate at the liquid-liquid interface which gradually disappear because of diffusion, this stage is called the nucleation period; And then a growth period starts after the disappearance of the interface.[26]

Hotta *et al.* studied the growth rate and the length of C_{60} nanowires prepared by LLIP method in various conditions to know their growth mechanism. They summarized that the growth rate of C_{60} nanowires is influenced remarkably by temperature and the degree of supersaturation, but scarcely by the diffusion of solutions, indicating that the growth is determined by the chemical reaction on the nanowire surface.[61, 62]

Zhou *et al.* proposed that the growth of C_{60} nanowires prepared by evaporation method using a C_{60} solution in 1,3,5-TMB follows a thin liquid film mechanism (Figure 27). A thin film of C_{60} solution is formed as the solution climbs up the inner wall of the reactor, and is maintained by the evaporation of the solvent and the continuous climb-up of the solution, and thus the concentration of C_{60} increases and becomes saturated at the top area of the film. Crystal seed of the C_{60}/1,3,5-TMB crystal forms and grows until the diameter of the crystal is larger than the thickness of the liquid film. Then the part exposed to air stops growing while the growth of the part in the liquid film continues, which pushes the protruded end outwards. Individual crystalline nanowires stand vertically to the surface of the film due to further crystal growth. In the meanwhile the hemispherical end of the crystal inside the liquid film grows in diameter. This mechanism can explain the driving force for the growth of the 1D C_{60} nanowires and the reason why the diameter of most of the as-prepared nanowires

varied from one end to another. However, the variation in diameter of the nanowires is found to be quite small because of the very thin liquid film and the high growth rate.[31]

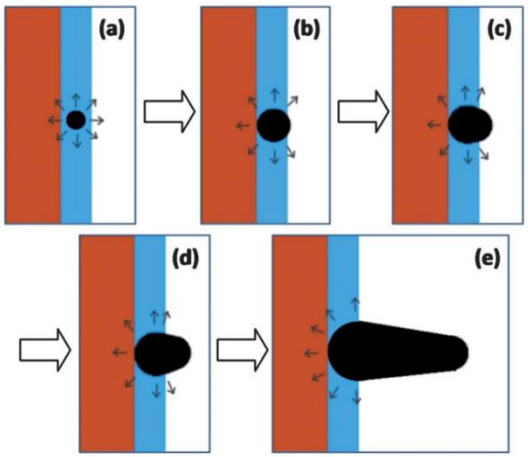

Figure 27. The growth of C_{60} nanowire due to the thin film evaporation mechanism.[31]

Geng *et al.* proposed a central growth mechanism to explain the growth of C_{60} nanowires with V- and Y-shaped cross sections.[10, 30] As shown in Figure 28(a), there was a short tip extruded at the end of a nanowire, which indicated that the growth was quicker at the centre of the nanowires than that of the wings. They concluded that the growth of the central core virtually led the overall growth of the crystals along the preferential one dimension, while side wings developed in directions perpendicular to the growth axis. They also suggested that the organic solvent as a guest species in the crystal structure plays an important role in the growth of C_{60} nanowires.

The authors also presented a view that the high boiling point of 1,2,4-TMB, ~168 °C, together with its high solubility to C_{60}, 33.5×10^{-4} M at 298 K, results in a prior solvation to the C_{60} molecules before the crystals grow. This view is in agreement with the observed phenomenon that all nanowires were found on the upper wall of the growth container instead of at the bottom, indicating that the growth of C_{60} nanowires was not from a conventional precipitation process from a supersaturated solution. Instead, the C_{60} molecules diffused with the solvent along the inner wall of the container, where the solvent vaporized and left the C_{60} molecules to nucleate.

To get a more in-depth understanding of the growth mechanism, Geng *et al.* studied the adhesion energy of a unit cell to evaluate the relative ease of the growth along three principal growth directions, *a*, *b* and *c* (Figure 28(b)) in different isomeric structures.[30] They found that the total energy of the unit cell and the relative adhesion energy along different growth directions largely depend on the location and orientation of 1,2,4-TMB molecules inside the crystal unit cell but little on the orientation of the C_{60} molecules. The adhesion energy along the *c* direction was found to be the highest, indicating that the growth along this direction was the most difficult, while the most favourable growth direction could be either *a* or *b* depending on the different isomeric state. However, the adhesion energy difference was

considerably large between the axis *a* and *b*, therefore, the crystal would preferably grow along one direction to form a 1-D shape.

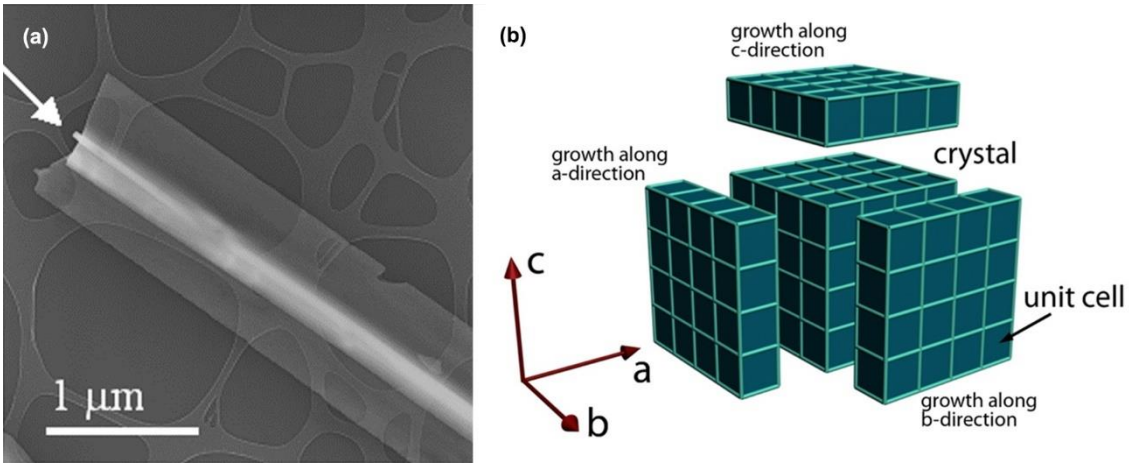

Figure 28. (a) TEM image of a short tip extruded at the end of a C_{60} nanowire. (b) A schematic diagram showing three principal growth directions of a C_{60} nanowire crystal.[30]

To understand the C_{60} nanowire growth mechanism in more details, Solov'yov *et al.* studied the influence of electron polarization on the growth anisotropy and the possible polymerization reactions occurring between the C_{60} and the solvent molecules.[63] The adhesion energy of a single fullerene molecule due to the polarization forces in the system was calculated to be ~10^{-4} eV, which is negligible since this energy is much smaller than the thermal vibration energy which is approximately 2.6×10^{-2} eV at room temperature. By comparing the C_{60} nanocrystals grown by using a series of polar solvents (toluene, 1,2,3-TMB and 1,2,4-TMB) and non-polar solvents (benzene, 1,3,5-TMB), they found that C_{60} nanowires were formed in both 1,2,4-TMB and 1,3,5-TMB while the crystallization in benzene, 1,2,3-TMB and toluene did not result in wire-like structure, which was in agreement with the above theoretical calculation, so a conclusion that the polarization effect can be neglected in the dynamical growth.

Yao *et al.* carried out detailed SEM studies on C_{60} nanowires prepared by evaporating a C_{60} solution in 1,3-dichlorobenzene on a substrate and observed some curious phenomenon.[29] As shown in Figure 29, two thin nanowires inserted into a bigger nanowire and left two holes in the nanowire which didn't close even though the growth continued. They suggested that the growth of C_{60} nanowires follows a nucleation-growth pathway and the preferable growth directions (2→1 and 2→3 in Figure 29) are parallel with the nucleation site (marked as 2 in Figure 29). They found that the solubility of C_{60} in solvents determined the size of nucleation site and thus the diameter of C_{60} nanowires, and suggested that the interaction of the aromatic solvent molecules with C_{60} molecules drives the formation of 1-D crystals.

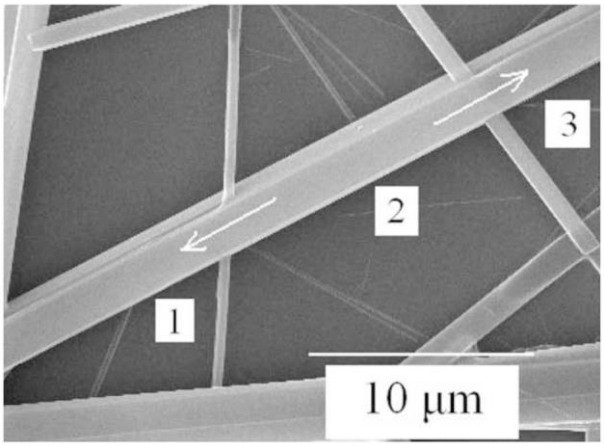

Figure 29. SEM image of a C_{60} wire growing along two opposite directions 2→1 and 2→3.[29]

As for the nanowire polymerization, Geng *et al.* observed that pristine C_{60} nanowires prepared by the evaporation method transformed into 1-D wire-like polymer after ageing for ~10 months.[48] They studied the mechanism of the polymerization progress, and suggested that the polymerization occurred following the nanowire growth until all 1,2,4-TMB molecules were covalently bonded to adjacent C_{60} molecules. Detailed theoretical analysis was carried out to try to get an in-depth understanding of the polymerization pathway. Based on both the experimental observation and theoretical calculation, they presented two possible polymerization scenarios: (i) two C_{60} molecules and a 1,2,4-TMB molecule to form two methylene bridges; (ii) three C_{60} molecules and a 1,2,4-TMB molecule to form three linkages. There are two possibilities of the first pathway with two possible products shown in Figure 30 (a) and (b):

$$C_{60} + TMB + C_{60} \rightarrow C_{60} - TMB^{-2H} - C_{60} + H_2 + \Delta E_1 \quad (1)$$

$$C_{60} + TMB + C_{60} \rightarrow HC_{60} - TMB^{-2H} - C_{60}H + \Delta E_2 \quad (2)$$

The reaction enthalpies of the two reactions were calculated to be ΔE_1 = 59.8 kcal mol^{-1} and ΔE_2 = −11.7 kcal mol^{-1}, respectively, indicating that reaction (2) is exothermic and energetically preferable (Figure 30 (a), (b)).

The second pathway can be written as below:

$$C_{60} + TMB + C_{60} + C_{60} \rightarrow 3C_{60}TMB + \Delta E_3 \quad (3)$$

The two possible structures of low-energy isomers of $3C_{60}$TMB are shown in Figure 30 (c) and (d). The reaction enthalpies for the two isomers (c) and (d) were calculated to be ΔE_3 = −53.64.8 kcal mol^{-1} and ΔE_3 = −55.11 kcal mol^{-1}, which implied that reaction (3) is exothermic and likely to occur in both cases.

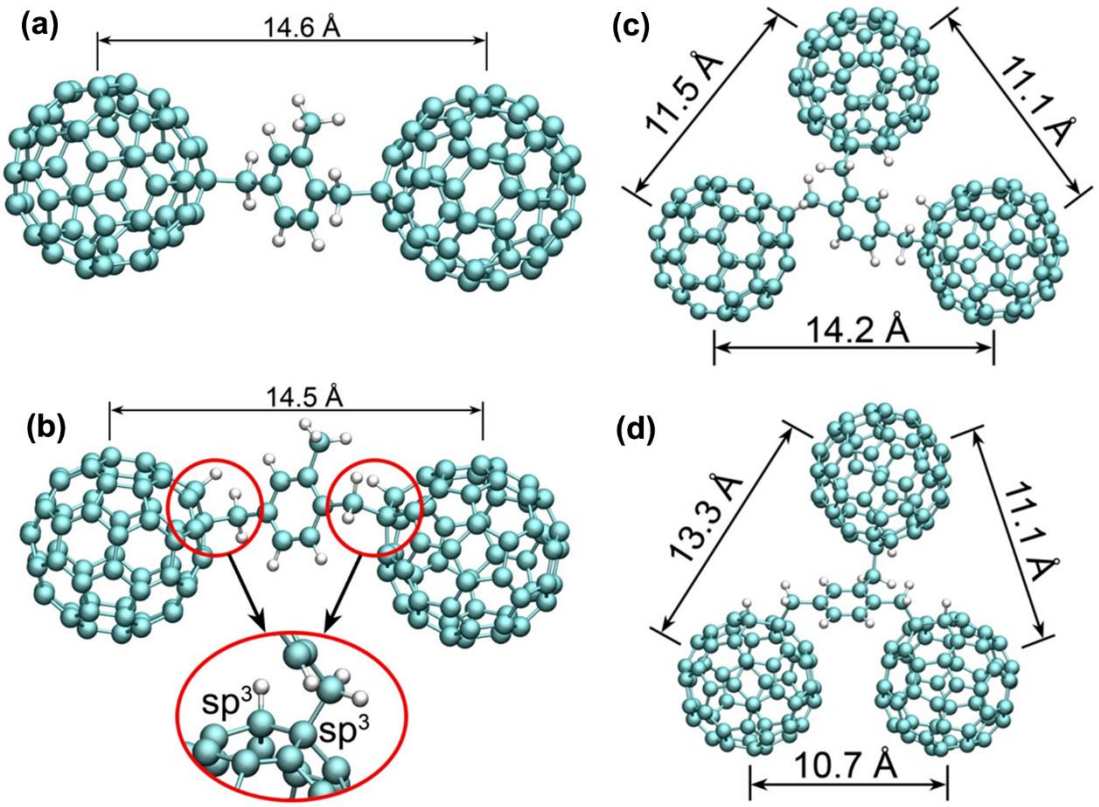

Figure 30. Structures of (a) C_{60}-TMB^{-2H}-C_{60} as the product of reaction (1), (b) HC_{60}-TMB^{-2H}-$C_{60}H$ as the product of reaction (2), and two low-energy isomers (c) and (d) of $3C_{60}TMB$ as the product of reaction (3).[53]

5. Applications of C_{60} nanowires

C_{60} nanowires maintain the interesting properties of C_{60} molecules, such as the nonlinear properties in the excited triplet state, photo-transformation properties and the strong bonding between C_{60} molecules and metal or Si surface,[4] therefore, they could have similar potential applications to that of C_{60} molecules. Besides, C_{60} nanowires also have special properties associated with the high surface area, low-dimensionality, and potential quantum confinement effect which make them potentially more widely applicable than C_{60} molecules. It is therefore expected that C_{60} nanowires could have potential applications in areas like optical limiters and photorefractive devices because of the intrinsically large magnitude of the nonlinear optical response of C_{60},[4, 5, 64] photo-electrical devices and photoconductors for solar energy devices because of their excellent photoinduced charge transfer properties,[2] fuel cells,[6, 55] field-emission transistors,[15, 16] nanoprobes,[17] high frequency filters,[17] free-standing membranes[65, 66] and sensors[4]. Remarkably, the material is also expected to find important biological and medical applications because of the simple carbon nature with only a small amount of hydrogen element in the structure.[10,53]

5.1 Optical applications

The unique optical properties of fullerene-related materials have been studied by numerous researchers and showed promise for optical applications. In a recent work carried out by Zheng *et al.*,[67] solution grown, large area C_{60} single crystal arrays were utilised as organic photodetectors which exhibit excellent UV-light sensing performance. Using a simple dip-coating process, heavily doped Si wafers with a 300 nm-thick SiO_2 dielectric layer were dipped vertically into a C_{60} solution (4 mg/ml in CS_2) and then removed at a constant speed ranging from 0.10 – 1.00 mm/min. The two terminal devices were fabricated via an electron beam lithography process in which Cr/Au (10 nm/50 nm) electrodes were deposited over the sample after a lift-off process via thermal evaporation. The photocurrent versus voltage (I-V) plots measured in dark and under illumination with lights of different wavelengths (as shown in Figure 31) reveal substantial photo-induced current generation under UV light illumination (350-400 nm) as compared to visible light irradiation (450–650 nm). Under a constant 400 nm illumination source, the device shows a photocurrent up to 7.3 pA ($\approx$1.822 mW cm^{-2}) versus a dark current of ~0.02 pA, displaying a large on/off ratio of 365. Consequently, the responsivity (Rλ), external quantum efficiency (EQE) and specific detectivity (D*) of this photodetector were determined to be 8.01 mA W^{-1}, 2.5 % and 7.08×10^8 Jones, respectively.

Comparatively, in a similar work carried out by Saran *et al.*,[68] C_{60} nanocrystals were prepared using a fast LLIP method employing CS_2 and IPA. As compared to C_{60} molecules, the C_{60} nanorods displayed a significantly broadened and extended absorption spectrum up to 750 nm with a significant redshift of ~100 nm attributed to the enhanced Coulombic interactions occurring between the C_{60} molecules in the solid phase. It is well established that C_{60} is an n-type semiconductor and the intercalation of oxygen introduces traps in the C_{60} molecule reducing its responsivity and sensitivity. Using Poly(3-hexylthiophene-2,5-diyl) (P3HT), Cadmium Selenide (CdSe) and Lead Sulphide (PbS) nanocrystals to achieve an ultralow photodoping mechanism, the authors showed enhanced (~ 400) photosensitivity of the devices. The excited photodopants were shown to fulfil two roles including: (i) filling of the trap states in the C_{60} nanorods *via* interfacial electron transfer and (ii) upon the filling of the trap states, the transferred electrons contributed to the overall photocurrent generation while the holes remained trapped in the photodopant. Consequently, the photodoped C_{60} nanowire photodetectors offered broadband UV-vis-NIR spectral tuneability, wherein the responsivity of the P3HT photodoped device was measured to be ~340 mAW^{-1}, with an EQE approaching ~100 % at 415 nm and D* of > 10^9 Jones, respectively. Thus, the high tuneable photosensitivity of the C_{60} nanowires extending across the visible spectrum demonstrates the potential of C_{60} nanorods in enabling devices such as photodetectors, photovoltaics as well as electrophotography.

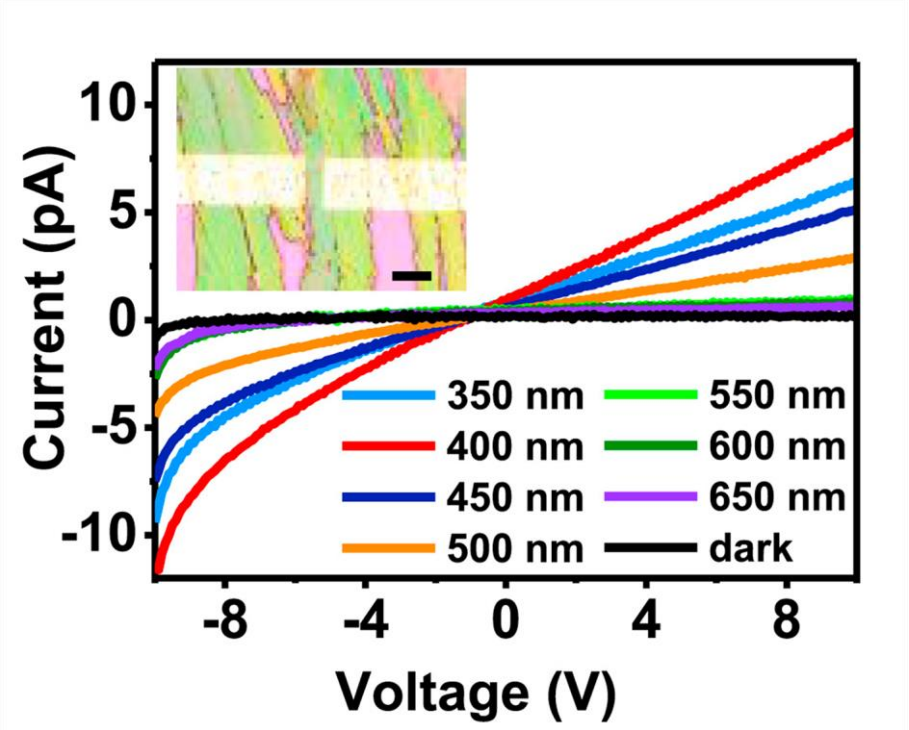

Figure 31. I-V curves of a C_{60} single-crystal array in dark and under illumination with different wavelengths at room temperature. Inserted is an optical image of the array with an exposure area of 50 mm^2, where the scale bar represents 10 mm.[67]

5.2 Electrical applications

Depending on the diameter, the electrical properties of C_{60} nanowires vary from insulator to semiconductor,[45] and as a consequence, the material can find potential electrical applications as insulator, low-dimensional semiconductors. In addition, C_{60} nanowires can be made into superconductors by doping with alkali metals such as potassium.[46, 69-72] Attempts have also been made to prepare metal/metal ion-containing C_{60} nanowires for the direct methanol fuel cells applications.[73]

Takeya and co-workers synthesized K-doped C_{60} nanowires (K_xC_{60}NW) which exhibited superconductivity at 17 K. The volume fraction was observed to be as high as 80% in $K_{3.3}C_{60}$ NW with a heat treatment at 200°C for 24 h, while the value of K-doped C_{60}, $K_{3.3}C_{60}$ which showed superconductivity at 19 K was lower than 1%. It was concluded that this significant difference in the fractions between K-doped C_{60} NW and K-doped C_{60} was due to the existence of disordered nanopores with an average size of 8.3 nm within the C_{60} nanowire structure formed during the drying process in the LLIP method which allowed an excessive amount of K over 3.0 to stay not only at the surface but also in the nanopores of C_{60} NWs.[72] These C_{60} nanowires could be utilized as flexible and lightweight superconducting wire owing to their unique wire-like structure.

Many attempts have been made to explain the superconducting mechanism in metal doped C_{60} system. One proposed theory involves Hubbard model,[74] which shows that the superconducting state is more stable than the charge density wave state in the fcc structure of K_3C_{60}. Another proposed mechanism for the same materials system is concerned with a parity doublet that triggers the superconducting transition.[75] It is noted that none of the theories are yet conclusive, due to lack of capacity to either accounting for many published experimental data or making systematic predictions for future experiments. Clearly, more research work is necessary in order to gain in-depth understanding of the superconducting mechanism.

Miyazawa *et al.* found that after a heat treatment at a temperature higher than 600 °C performed on C_{60} nanowires prepared by LLIP method, C_{60} shell tubes with both open ends and closed spherical ends were formed. They also synthesized C_{60} shell tubes by heating the C_{60} nanowires prepared using C_{60} powders containing $(\eta_2\text{-}C_{60})Pt(PPh_3)$ at 900°C. The specific surface area of these C_{60} shell tubes was measured to be 380 $m^2\ g^{-1}$ using BET method. Although the electrical resistance of C_{60} wires was very high ($>10^5$ Ω·cm), the conductivity was notably improved after the heat treatment, for example, the resistivity value of a C_{60} wire with a diameter of 2.2 μm was measured to be 0.037 Ω·cm. These high temperature-treated C_{60} nanowires were proposed for use as new electrode materials for fuel cells because of their high specific surface area and excellent electrical conductivity.[55]

Field effect transistor (FET) is another important electrical application for C_{60} nanomaterials.[68] Ogawa successfully fabricated C_{60}-nanowire-based FETs whose semiconducting channel is formed by a large number of C_{60} nanowire crystals with diameters less than 300 nm and lengths more than 100 μm. The C_{60}-nanowire-based FETs were found to exhibit n-channel, normally-on properties, and their carrier mobility was estimated to be 2×10^{-2} cm^2/Vs at room temperature in vacuum. It can be expected that C_{60} nanowires are promising for realizing high-mobility organic FETs.[16] However, most C_{60}-based electrical devices are not suitable to use directly in the air because dioxygen may diffuse into the interstitial sites of the fullerene solid. Therefore, it is necessary to coat C_{60} materials with oxygen-resistant materials to prevent oxidation when C_{60} devices are to be commercialized.[4, 76, 77]

5.3 Mechanical devices

The superior properties of fullerene materials have also been utilized in mechanical and electromechanical devices.[78] For use in mechanical structures, they should be formed as free-standing structures, such as cantilever or doubly supported beams and membranes, rather than fixed on the substrates.[65] Much effort has been made on the research of fabrication or assembly process of carbon nanomaterials on a substrate by controlling their position and dimensions. However, a great deal of issues remain in realizing MEMS devices with fullerene nanomaterials, for example, the fabrication process of the devices is difficult and the properties database essential for device designing is still incomplete.[66]

Tsuchiya and co-workers reported a two-step process including direct electron beam writing and sacrificial dry etching for the fabrication of doubly-supported free-standing C_{60} nanowires on a capacitive MEMS system as mechanical sensor for on-chip nanoscale tensile testing. Polymerized C_{60} nanowires were patterned by irradiating vacuum-deposited C_{60} film with an electron beam and then released using silicon as a sacrificial layer and XeF_2 as an etchant gas at a pressure of 10 Pa to form free-standing C_{60} nanowires on silicon beam structures.[65, 66] The free-standing C_{60} nanowire at the resist opening was 2 μm in length, 400 nm in width and 15 nm in thickness. The fabrication process can also be applied to various C_{60}-nanostructure-related devices.

Néel *et al*. fabricated long and narrow C_{60} nanowires onto a vicinal Au (433) surface.[79] The fabrication process included the deposition of 0.5 monolayer C_{60} on Au (433) and a subsequent annealing treatment at a temperature of 500 K. The resulting surface exhibits alternating metal (111) and fullerene stripes (533). While the width of the stripes corresponds to an average of six adjacent molecule chains, the length of the stripes reaches several hundreds of nanometers. This surface morphology is expected to be utilized as a template for subsequent deposition of functional units which preferentially bond to the fullerene molecules. The authors tentatively attributed the driving force to the minimization of the free energy of the substrate facets induced by the combined effect of C_{60} adsorption and annealing. This type of research work is related to the fabrication of nanostructures exploiting surface stress, which is expected to play a crucial role in fabricating devices with highly uniform and predictable electrical, magnetic, or optical properties.[79]

5.4 Biological applications

Various functionalized fullerenes and nanocarbons have yielded promising applications in bio-medicinal fields such as drug delivery, reactive oxygen species quenching[18-20], targeted imaging[80] and tissue engineering[81-84] due to their chemical and physical properties. The photosensitivity of fullerenes makes them good candidates for photodynamic therapy of cancer and treatment of multidrug resistant pathogens.[85, 86] It was reported that fullerenes have a potential as biological antioxidants with advantages of their ability to localize within the cell to mitochondria and other cell compartment sites, where in diseased states, the production of free radicals takes place.[87] Because fullerenes possess large amount of conjugated double bonds and low lying lowest unoccupied molecular orbital (LUMO) which can easily take up an electron, an attack by radical species is highly possible. Fullerenes can react with many superoxides without being consumed, therefore, they are considered to be the most efficient radical scavenger in the world.[18] Fullerenes and their derivatives also have potential antiviral activity based on their biological properties including the unique molecular architecture and antioxidant activity, which makes them promising for implications on the treatment of human immunodeficiency virus (HIV)-infection.[88]

Minani *et al.* developed tetra(piperazino)fullerene epoxide (TPFE), a water-soluble cationic tetraamino fullerene, as carrier vehicle in blood vessels to build a lung-selective

delivery system of small interfering RNA (siRNA).[89] Since fullerene-polymer nanowires can take advantage of the biologically important properties of fullerenes, they are believed to have availability in aforementioned aspects. Other nanocarbons such as carbon nanotubes and graphene have also been applied to biological fields. Carbon nanotubes can be easily internalized by cells, and therefore can act as delivery vehicles for a variety of molecules relevant to therapy and diagnosis.[90] They are considered as promising nano-carriers for the delivery of various anticancer and non-anticancer drugs, owing to their high surface area, enhanced cellular uptake and the possibility to be easily conjugated with many therapeutics, including both small molecules and biologics, displaying superior efficacy, enhanced specificity and diminished side effects.[91-93]

Different from the growth of carbon nanotubes catalysed by metal nanoparticles which cannot be removed completely by post-purification processes,[10, 53, 94] the preparation process of polymerized C_{60} nanowires is totally metal-free and the material is composed almost entirely of carbon, and thus its biocompatibility is improved remarkably. It is suggested that the tissue-compatible and biocompatible material with low cytotoxicity[88, 95, 96] promises potential applications in biomedicinal fields including drug delivery, biosensor preparation, diagnosis and treatment of major ailments such as cancer,[97] heart,[98] lung,[89] and blood diseases.[99] This might be applicable as a cellular scaffold suitable for inducing myogenic differentiation with concurrent control of the growth direction of cells,[82] which may be more attractive than carbon nanotubes. However, there are some limitations to the application of fullerene nanowires in biological system since this nanomaterial lacks good solubility in biologically relevant media[100-102] and it is not well biodegradable. One possible way to solve this problem and help to achieve the goals of biological applications is to combine fullerene nanowires with other biomaterials.

5.5 Electrochemical applications

Fullerene, as an important member of carbon family, promises many applications in chemical, electrochemical, and other energy related applications together with other members of the same family such as graphite, carbon nanotubes, graphene, diamond, and activated amorphous carbon.[4, 103, 104] C_{60} molecules, with their conjugated π bonding and excellent electron acceptor capability, could accelerate electron transfer while free of any metallic impurities. This makes fullerene beset carbon nanotubes, and as such, the material could be used for a variety of electrochemical sensing media. The issues around the aggregation and inhibition of redox activity of C_{60} especially in aqueous media has been overcome by covalent functionalization using carboxyl, hydroxyl, amine groups as well as via non-covalent supramolecular interactions thus making C_{60} molecules water soluble for electrochemical biosensing. It should be mentioned that there has been significant debate on the origins of superior electrocatalytic activity in C_{60} films, where the opinion has ranged from C_{60} being highly effective in electrocatalysis to "thin-layer effects" arising from the porosity of the C_{60} films on glassy electrodes. Nevertheless, the purported electrochemical properties of C_{60} including multiple redox states, stability in many redox states and ease of

functionalization have been extensively used as a mediator between the recognition site and electrode in catalytic biochemical sensors.

As is the case with the other physical properties, a significant difference was observed in the electrochemical properties of the C_{60} and the C_{60} nanowires. In one of the studies carried out by Zhang *et al.*,[105] two sandwich-type electrodes consisting of C_{60} or C_{60} nanowires interlayer covered by a room temperature ionic liquid (RTIL) membrane on single-walled carbon nanotubes (SWNTs) modified glassy carbon electrode (GCE) surface were fabricated. The thus obtained RTIL/C_{60}/SWNT/GCE and RTIL/C_{60} nanowire/SWNT/GCE were analyzed in a 0.2 M Britton-Robinson (B–R) buffer solution of pH 7.0 using cyclic voltammetry and differential pulse voltammetry. It was observed that within the potential scan window, 4 pairs of quasi-reversible redox peaks occurred at the RTIL/C_{60}/SWNT/GCE, while only two peaks were observed for the RTIL/C_{60} nanowire/SWNT/GCE. For the C_{60} electrode, quasi-reversible multiple-step electron-transfer reactions were described as following:

$$C_{60} \overset{e-}{\Leftrightarrow} C_{60} \overset{e-}{\Leftrightarrow} {C_{60}}^{2-} \overset{e-}{\Leftrightarrow} {C_{60}}^{3-} \overset{e-}{\Leftrightarrow} {C_{60}}^{4-}$$

Whereas for the RTIL/C_{60} nanowire/SWNT/GCE, the C_{60} nanowires could not be oxidised again in the reverse scan and the electrode process was deemed to be irreversible under the experimental conditions. Accordingly, the possible mechanism of the electrode process was described as the following:

$$C_{60\ nanowire} \overset{e-}{\Leftrightarrow} {C_{60\ nanowire}}^{-} \overset{e-}{\Leftrightarrow} {C_{60\ nanowire}}^{2-}$$

It was assumed that the electrons accumulated by fullerene nanowires were difficult to be released again presumably due to the 1-D nature of the nanowire. The influence of the scan rate on the electrochemical responses was further studied with CV and the result showed that the electrochemical reaction was also adsorption-controlled processes unlike the diffusion-controlled process observed for most of the other carbon-based electrodes.[105]

With respect to C_{60} nanowires, Zhang *et al.* developed sequence specific single-stranded DNA complexes with C_{60} nanowires to obtain a film like structure for electrochemical sensing of dopamine in the presence of ascorbic acid. The interactions between the C_{60} nanowires and DNA was confirmed to be of π–π stacking and hydrophobic interaction type. The C_{60} nanowire/DNA electrode in the B-R buffer solution again showed only reductive peaks and no oxidative peaks at all, thus implying that when the reduced electrode modified with C_{60} nanowire/DNA was used as the working electrode to analyze any other electroactive molecules, no other peaks showed up. Thus, the negatively charged electrode showed two attractive advantages: they were free of interfering peak in a rather wide window and strong effect on analyte due to electrostatic interaction.[106]

In a more recent work, Wakahara *et al.* studied the electrochemical properties of C_{60} nanowires to enable the oxygen reduction reaction (ORR) in aqueous solutions.[107] Utilising nanoporous C_{60} nanowires prepared using LLIP method with a specific surface area of 376 m^2/g, the GCE electrodes with Nafion, Nafion C_{60} nanowires and Nafion-C_{60} powder were

measured in Ar- or O_2-saturated 0.10 M KOH solution in a potential range from 0.0 to -1.0 V vs. SCE. The reduction peak for oxygen was observed to be around -0.45V corresponding to the less than ideal one-electron processes for the reduction of O_2 to superoxide $O_2^{\cdot-}$. As compared to the pristine C_{60} powders and GCE, a significant ORR catalytic activity for the C_{60} nanowires was observed in the basic media thereby indicating that the physical properties of good electrical conductivity, high surface area and absorption of oxygen in the case of C_{60} nanowires are of utmost importance.

6. Summary

In this review, we have first discussed the direct evaporation method and LLIP method for growing C_{60} nanowires. The LLIP method is widely used for the purpose of preparation, but the product contains C_{60} nanocrystals of various shapes and sizes and currently there is still lack of separation method. Using the direct evaporation method, people may grow long C_{60} nanowires with good quality. However, the evaporation process is normally slow, the method may not be ideal for commercial production of the material. The characterization techniques highlighted here have proven to be very useful to study the morphology, crystalline structure, chemical composition, mechanical properties, and even biological properties of this novel carbon. To get better and in-depth understanding of the growth process of C_{60} nanowires, detailed research work on both experiments and theoretical modelling is still necessary. Given the outstanding properties of C_{60} nanowires associated to their high surface area, low-dimensionality and potential quantum confinement effect, it is reasonable to believe that the material will find a wide range of applications in the future for both scientific research and technological innovations.

References

1. H. W. Kroto, J. R. Heath, S. C. O'Brien, R. F. Curl and R. E. Smalley, *Nature*, 1985, **318**, 162-163.
2. N. Sariciftci, L. Smilowitz, A. J. Heeger and F. Wudl, *Science*, 1992, **258**, 1474-1476.
3. P. R. Somani, S. P. Somani and M. Umeno, *Applied Physics Letters*, 2007, **91**, 173503-173503.
4. M. S. Dresselhaus, G. Dresselhaus and P. C. Eklund, *Science of fullerenes and carbon nanotubes: their properties and applications*, Academic press, 1996.
5. L. W. Tutt and T. F. Boggess, *Progress in quantum electronics*, 1993, **17**, 299-338.
6. M. Sathish and K. i. Miyazawa, *CrystEngComm*, 2010, **12**, 4146.
7. S. H. Friedman, D. L. DeCamp, R. P. Sijbesma, G. Srdanov, F. Wudl and G. L. Kenyon, *Journal of the American Chemical Society*, 1993, **115**, 6506-6509.
8. R. Schinazi, R. Sijbesma, G. Srdanov, C. Hill and F. Wudl, *Antimicrobial agents and chemotherapy*, 1993, **37**, 1707-1710.
9. R. Sijbesma, G. Srdanov, F. Wudl, J. Castoro, C. Wilkins, S. H. Friedman, D. L. DeCamp and G. L. Kenyon, *Journal of the American Chemical Society*, 1993, **115**, 6510-6512.
10. J. Geng, W. Zhou, P. Skelton, W. Yue, I. A. Kinloch, A. H. Windle and B. F. Johnson, *Journal of the American Chemical Society*, 2008, **130**, 2527-2534.

11. L. K. Shrestha, Q. Ji, T. Mori, K. i. Miyazawa, Y. Yamauchi, J. P. Hill and K. Ariga, *Chem. Asian J*, 2013, **8**, 1662-1679.
12. C. M. Lieber and Z. L. Wang, *MRS bulletin*, 2007, **32**, 99-108.
13. W. Guss, J. Feldmann, E. O. Gobel, C. Taliani, H. Mohn, W. Muller, P. Haussler and H. ter Meer, *Physical review letters*, 1994, **72**, 2644-2647.
14. R. Saito, G. Dresselhaus and M. Dresselhaus, *Physical Review B*, 1992, **46**, 9906.
15. J. Kastner, J. Paloheimo and H. Kuzmany, *Fullerene field-effect transistors*, Springer, 1993.
16. K. Ogawa, T. Kato, A. Ikegami, H. Tsuji, N. Aoki, Y. Ochiai and J. P. Bird, *Applied Physics Letters*, 2006, **88**, 112109.
17. S.-H. Lee, K. i. Miyazawa and R. Maeda, *Carbon*, 2005, **43**, 887-889.
18. P. Krusic, E. Wasserman, P. Keizer and I. Morton, *Science*, 1991, **254**, 1183.
19. R. M. Lucente-Schultz, V. C. Moore, A. D. Leonard, B. K. Price, D. V. Kosynkin, M. Lu, R. Partha, J. L. Conyers and J. M. Tour, *Journal of the American Chemical Society*, 2009, **131**, 3934-3941.
20. J.-J. Yin, F. Lao, P. P. Fu, W. G. Wamer, Y. Zhao, P. C. Wang, Y. Qiu, B. Sun, G. Xing and J. Dong, *Biomaterials*, 2009, **30**, 611-621.
21. K. Miyazawa, Y. Kuwasaki, K. Hamamoto, S. Nagata, A. Obayashi and M. Kuwabara, *Surface and Interface Analysis*, 2003, **35**, 117-120.
22. K. Miyazawa, Y. Kuwasaki, A. Obayashi and M. Kuwabara, *Journal of Materials Research*, 2002, **17**, 83-88.
23. K. Miyazawa, C. Nishimura, M. Fujino, T. Suga and T. Yoshii, *TRANSACTIONS-MATERIALS RESEARCH SOCIETY OF JAPAN*, 2004, **29**, 1965-1968.
24. K. i. Miyazawa and K. Hotta, *Journal of Crystal Growth*, 2010, **312**, 2764-2770.
25. M. Sathish and K. Miyazawa, *Molecules*, 2012, **17**, 3858-3865.
26. M. Tachibana, K. Kobayashi, T. Uchida, K. Kojima, M. Tanimura and K. Miyazawa, *Chemical Physics Letters*, 2003, **374**, 279-285.
27. S. Ogawa, H. Furusawa, T. Watanabe and H. Yamamoto, *Journal of Physics and Chemistry of solids*, 2000, **61**, 1047-1050.
28. L. Wang, B. Liu, D. Liu, M. Yao, Y. Hou, S. Yu, T. Cui, D. Li, G. Zou, A. Iwasiewicz and B. Sundqvist, *Advanced Materials*, 2006, **18**, 1883-1888.
29. M. Yao, B. M. Andersson, P. Stenmark, B. Sundqvist, B. Liu and T. Wågberg, *Carbon*, 2009, **47**, 1181-1188.
30. J. Geng, I. A. Solov'yov, W. Zhou, A. V. Solov'yov and B. F. Johnson, *The Journal of Physical Chemistry C*, 2009, **113**, 6390-6397.
31. Y. Zhou and W. Zhou, *CrystEngComm*, 2012, **14**, 1449-1454.
32. M. Sathish, K. i. Miyazawa, J. P. Hill and K. Ariga, *Journal of the American Chemical Society*, 2009, **131**, 6372-6373.
33. J.-i. Minato and K. i. Miyazawa, *Carbon*, 2005, **43**, 2837-2841.
34. A. Aota, A. Hibara and T. Kitamori, *Analytical chemistry*, 2007, **79**, 3919-3924.
35. K. i. Miyazawa, C. Hirata and T. Wakahara, *Journal of Crystal Growth*, 2014, **405**, 68-72.
36. G. Chambers and H. Byrne, *Chemical physics letters*, 1999, **302**, 307-311.
37. K. Matsuishi, T. Ohno, N. Yasuda, T. Nakanishi, S. Onari and T. Arai, *Journal of Physics and Chemistry of Solids*, 1997, **58**, 1747-1752.
38. M. Matus and H. Kuzmany, *Applied Physics A*, 1993, **56**, 241-248.
39. A. M. Rao, P. Zhou, K.-A. Wang, G. Hager, J. Holden, Y. Wang, W.-T. Lee, X.-X. Bi, P. Ecklund and D. Cornett, *Science*, 1993, **259**, 955-957.
40. M. Tachibana, H. Sakuma, T. Komatsu and K. Kojima, Optical Science, Engineering and Instrumentation'97, 1997.
41. I. Manika, J. Maniks, R. Pokulis, J. Kalnacs and D. Erts, *physica status solidi (a)*, 2001, **188**, 989-998.

42. S. Malik, N. Fujita, P. Mukhopadhyay, Y. Goto, K. Kaneko, T. Ikeda and S. Shinkai, *J. Mater. Chem.*, 2007, **17**, 2454-2458.
43. R. Kato and K. i. Miyazawa, *Journal of Nanotechnology*, 2012, **2012**.
44. K. i. Miyazawa, M. Fujino, J.-i. Minato, T. Yoshii, T. Kizuka and T. Suga, Smart Materials III, 2004.
45. T. Konno, T. Wakahara and K. i. Miyazawa, *Journal of Crystal Growth*, 2015, **416**, 41-46.
46. H. Takeya, R. Kato, T. Wakahara, K. i. Miyazawa, T. Yamaguchi, T. Ozaki, H. Okazaki and Y. Takano, *Materials Research Bulletin*, 2013, **48**, 343-345.
47. D. S. Bethune, G. Meijer, W. C. Tang, H. J. Rosen, W. G. Golden, H. Seki, C. A. Brown and M. S. de Vries, *Chemical physics letters*, 1991, **179**, 181-186.
48. Y. Iwasa, T. Arima, R. Fleming, T. Siegrist, O. Zhou, R. Haddon, L. Rothberg, K. Lyons, H. Carter and A. Hebard, *Science*, 1994, **264**, 1570-1572.
49. B. Sundqvist, *Advances in Physics*, 1999, **48**, 1-134.
50. K.-A. Wang, Y. Wang, P. Zhou, J. Holden, S.-l. Ren, G. Hager, H. Ni, P. Eklund, G. Dresselhaus and M. Dresselhaus, *Physical Review B*, 1992, **45**, 1955.
51. K. Calamba, C. Ringor, C. Pascua and K. i. Miyazawa, *Fullerenes, Nanotubes and Carbon Nanostructures*, 2015, **23**, 709-714.
52. M. Watanabe, K. Hotta, K. Miyazawa and M. Tachibana, Journal of Physics: Conference Series, 2009.
53. J. Geng, I. A. Solov'yov, D. G. Reid, P. Skelton, A. E. Wheatley, A. V. Solov'yov and B. F. Johnson, *Physical Review B*, 2010, **81**, 214114.
54. A. Rao, P. Eklund, U. Venkateswaran, J. Tucker, M. Duncan, G. Bendele, P. Stephens, J.-L. Hodeau, L. Marques and M. Nunez-Regueiro, *Applied Physics A*, 1997, **64**, 231-2239.
55. K. i. Miyazawa, J.-i. Minato, H. Zhou, T. Taguchi, I. Honma and T. Suga, *Journal of the European Ceramic Society*, 2006, **26**, 429-434.
56. K. Asaka, R. Kato, K. i. Miyazawa and T. Kizuka, *Applied physics letters*, 2006, **89**, 071912.
57. M. Larsson and S. Lucyszyn, Journal of Physics: Conference Series, 2009.
58. M. Larsson, J. Kjelstrup-Hansen and S. Lucyszyn, *ECS Transactions*, 2007, **2**, 27-38.
59. K. i. Miyazawa, *Science and technology of advanced materials*, 2015, **16**, 013502.
60. H.-X. Ji, J.-S. Hu, L.-J. Wan, Q.-X. Tang and W.-P. Hu, *Journal of Materials Chemistry*, 2008, **18**, 328-332.
61. K. Hotta and K. Miyazawa, Journal of Physics: Conference Series, 2009.
62. K. Hotta and K. I. Miyazawa, *Nano*, 2008, **3**, 355-359.
63. I. A. Solov'yov, J. Geng, A. V. Solov'yov and B. F. Johnson, Conf. Series 17th Symp. on Atomic, Cluster and Surface Physics SASP2010, Obergurgl, Austria, 2010.
64. L. W. Tutt and A. Kost, 1992.
65. T. Tsuchiya, Y. Ura, T. Jomori, K. Sugano and O. Tabata, *Journal of Micro/Nanolithography, MEMS, and MOEMS*, 2009, **8**, 013020-013020-013026.
66. T. Tsuchiya, T. Jomori, Y. Ura, K. Sugano and O. Tabata, Micro Electro Mechanical Systems, 2008. MEMS 2008. IEEE 21st International Conference on, 2008.
67. S. Zheng, X. Xiong, Z. Zheng, T. Xu, L. Zhang, T. Zhai and X. Lu, *Carbon*, 2018, **126**, 299-304.
68. R. Saran, V. Stolojan and R. J. Curry, *Scientific reports*, 2014, **4**, 5041.
69. A. Hebard, M. Rosseinky, R. Haddon, D. Murphy, S. Glarum, T. Palstra, A. Ramirez and A. Karton, *Nature*, 1991, **350**, 600-601.
70. T. Makarova, *Semiconductors*, 2001, **35**, 243-278.
71. R. F. Service, *Science*, 2001, **293**, 1570-1570.
72. H. Takeya, K. Miyazawa, R. Kato, T. Wakahara, T. Ozaki, H. Okazaki, T. Yamaguchi and Y. Takano, *Molecules*, 2012, **17**, 4851-4859.
73. M. Sathish, K. Miyazawa and T. Sasaki, *Journal of Solid State Electrochemistry*, 2007, **12**, 835-840.
74. F. Zhang, M. Ogata and T. Rice, *Physical review letters*, 1991, **67**, 3452.

75. R. Friedberg, T. Lee and H. Ren, *Physical Review B*, 1992, **46**, 14150.
76. P. Zhou, A. M. Rao, K. A. Wang, J. Robertson, C. Eloi, M. S. Meier, S. Ren, X. X. Bi, P. Eklund and M. Dresselhaus, *Applied physics letters*, 1992, **60**, 2871-2873.
77. C. C. Eloi, D. J. Robertson, A. M. Rao, P. Zhou, K. Wang and P. C. Eklund, *Journal of materials research*, 1993, **8**, 3085-3089.
78. C. Hierold, TRANSDUCERS 2007-2007 International Solid-State Sensors, Actuators and Microsystems Conference, 2007.
79. N. Néel, J. Kröger and R. Berndt, *Applied Physics Letters*, 2006, **88**, 163101.
80. G. Lucignani, *European journal of nuclear medicine and molecular imaging*, 2009, **36**, 869-874.
81. B. S. Harrison and A. Atala, *Biomaterials*, 2007, **28**, 344-353.
82. K. Minami, Y. Kasuya, T. Yamazaki, Q. Ji, W. Nakanishi, J. P. Hill, H. Sakai and K. Ariga, *Advanced Materials*, 2015, **27**, 4020-4026.
83. W. Nakanishi, K. Minami, L. K. Shrestha, Q. Ji, J. P. Hill and K. Ariga, *Nano Today*, 2014, **9**, 378-394.
84. S. Ryu, C. Lee, J. Park, J. S. Lee, S. Kang, Y. D. Seo, J. Jang and B. S. Kim, *Angewandte Chemie*, 2014, **126**, 9367-9371.
85. O. Stoilova, C. Jérôme, C. Detrembleur, A. Mouithys-Mickalad, N. Manolova, I. Rashkov and R. Jérôme, *Chemistry of materials*, 2006, **18**, 4917-4923.
86. O. Stoilova, C. Jérôme, C. Detrembleur, A. Mouithys-Mickalad, N. Manolova, I. Rashkov and R. Jérôme, *Polymer*, 2007, **48**, 1835-1843.
87. A. Kumar, *Journal of Environmental and Applied Biosearch*, 2015, **3**, 175-191.
88. R. Bakry, *International Journal of Nanomedicine*, 2007, **2**, 639-649.
89. K. Minami, K. Okamoto, D. Kent, K. Harano, E. Noiri and E. Nakamura, *Scientific reports*, 2014, **4**.
90. K. Kostarelos, A. Bianco and M. Prato, *Nature nanotechnology*, 2009, **4**, 627-633.
91. S. Goenka, V. Sant and S. Sant, *Journal of Controlled Release*, 2014, **173**, 75-88.
92. R. Singh and S. V. Torti, *Advanced drug delivery reviews*, 2013, **65**, 2045-2060.
93. B. S. Wong, S. L. Yoong, A. Jagusiak, T. Panczyk, H. K. Ho, W. H. Ang and G. Pastorin, *Advanced drug delivery reviews*, 2013, **65**, 1964-2015.
94. J. Geng, I. A. Kinloch, C. Singh, V. B. Golovko, B. F. Johnson, M. S. Shaffer, Y. Li and A. H. Windle, *The Journal of Physical Chemistry B*, 2005, **109**, 16665-16670.
95. J. Okuda-Shimazaki, S. Takaku, K. Kanehira, S. Sonezaki and A. Taniguchi, *International journal of molecular sciences*, 2010, **11**, 2383-2392.
96. S. Yamago, H. Tokuyama, E. Nakamura, K. Kikuchi, S. Kananishi, K. Sueki, H. Nakahara, S. Enomoto and F. Ambe, *Chemistry & biology*, 1995, **2**, 385-389.
97. J. LaRocque, D. J. Bharali and S. A. Mousa, *Molecular biotechnology*, 2009, **42**, 358-366.
98. P. Schoenhagen and J. L. Conyers, *Recent patents on cardiovascular drug discovery*, 2008, **3**, 98-104.
99. D. B. Buxton, *Nanomedicine*, 2009, **4**, 331-339.
100. R. Partha and J. L. Conyers, *International journal of nanomedicine*, 2009, **4**, 261.
101. R. Ruoff, D. S. Tse, R. Malhotra and D. C. Lorents, *The Journal of Physical Chemistry*, 1993, **97**, 3379-3383.
102. N. Sivaraman, R. Dhamodaran, I. Kaliappan, T. Srinivasan, P. V. Rao and C. Mathews, *The Journal of Organic Chemistry*, 1992, **57**, 6077-6079.
103. W. Zhang, X. Jiang, X. Wang, Y. V. Kaneti, Y. Chen, J. Liu, J. S. Jiang, Y. Yamauchi and M. Hu, *Angewandte Chemie International Edition*, 2017, **56**, 8435-8440.
104. H. Tian, J. Liang and J. Liu, *Advanced Materials*, 2019, **31**, 1903886.
105. X. Zhang, K. Jiao, G. Piao, S. Liu and S. Li, *Synthetic Metals*, 2009, **159**, 419-423.
106. X. Zhang, Y. Qu, G. Piao, J. Zhao and K. Jiao, *Materials Science and Engineering: B*, 2010, **175**, 159-163.
107. T. Wakahara, M. Sathish, K. i. Miyazawa and O. Ito, *Fullerenes, Nanotubes and Carbon Nanostructures*, 2015, **23**, 509-512.

Xiao Fan received her MSc degree from Jiangsu Normal University, China, in 2015. She is currently a PhD student at the University of Bolton. Her research interests include fullerene-related carbon nanomaterials and their biochemical applications.

Navneet Soin is a Lecturer at the School of Engineering, Ulster University, UK. He obtained his PhD from NIBEC, Ulster University in 2012. His research interests include development of materials and structures for energy harvesting, nanostructured carbon materials for electrochemical energy devices, plasma modification of high-performance polymers and technical textiles. He has over 50 peer-reviewed publications, has written 4 book chapters and currently holds two patents.

Haitao Li is a professor currently in the School of Chemical and Materials Science at Jiangsu Normal University, China. He did his Ph. D Degree under the supervision of Professor Anders Lund in Physical Chemistry at Linkoping University, Sweden. He was then doing Principal Investigator with Prof. David Klenerman in the Department of Chemistry at the University of Cambridge, UK. His research interests are the development and application of novel biophysical methods to biological and biomedical problems. This includes single molecule fluorescence spectroscopy of individual molecules, bio-nanotechnology and nanomaterials. He is one of the co-authors of over 80 papers and 10 patents. He also founded Deep-Blue, a graphene company.

Hua Li is an associate professor at the college of life and environmental sciences, Minzu University of China. She obtained her PhD from State Key Lab of Inorganic Synthesis and Preparative Chemistry, Jilin University in 2007. Her research interests focus on the synthesis

of functional nanomaterials, ranging from fundamental research to their application on energy and environment. She has over 30 peer-reviewed publications, and written 1 book.

_____

Xiaohong Xia received her PhD degree from the Central China Normal University in June 2007. She worked at the University of Bolton as a visiting scientist and then worked as a postdoctoral research fellow in 2010–2011. She is currently a professor of materials at Hubei University. Her current research interest is design and fabrication of semiconductor materials and devices (gas sensors, batteries, photocatalysis).

Junfeng Geng is a Reader in Materials Chemistry, University of Bolton. He received his PhD degree (Physical Chemistry) from the Department of Chemistry, University of Cambridge. His research interests are of inorganic and polymeric nanomaterials including chemical synthesis, property characterization, and industrial applications. He is the author of over 100 publications mainly as full, refereed original research papers published at international chemistry and materials science journals. He has made a number of scientific discoveries and technical inventions, including 12 patents filed up at UK national, European and International levels in the field of metal catalysts and carbon nanomaterials. Several of his inventions have been successfully commercialized in the UK into market products.

His research interests are in the field of material chemistry and nanotechnology. These include (1) Synthesis and characterisation of transition metal nanoparticles and molecular nanoclusters; (2) Growth and property studies of carbon nanotubes and graphene; (3) Synthesis and characterisation of inorganic and fullerene-based nanowires; (4) Metal nanoparticles for catalysis and electronic device applications; (5) Inorganic and polymeric nanomaterials for applications in chemical composites, renewable energy, and environmental clean technologies.